University of Stavanger

FACULTY OF SCIENCE AND TECHNOLOGY

MASTER'S THESIS

Curriculum: Biological Chemistry	Autumn/Spring semester, 2018/2019 Open
Author: Charlotte Bärbel Wiemann	Charlotte Wiemann ..... (author signature)

Supervisor: Daniela Pampanin

External Supervisor: Andrea Bagi

Master thesis title: Development of a portable surface plasmon resonance based genosensor for the detection of obligate hydrocarbon degrading bacteria in the marine environment

Keywords: Surface plasmon resonance; Oleispira antarctica; 16S rRNA; biosensor; environmental sample processor	Number of pages: 57 + appendices/other: 10 Stavanger, 01.06.2019 date/year

UNIVERSITY OF STAVANGER

MASTER'S THESIS

Development of a portable surface plasmon based genosensor for the detection of obligate hydrocarbon degrading bacteria in the marine environment

Author:
Charlotte Wiemann

Supervisor:
Daniela Pampanin

A thesis submitted in fulfillment of the requirements for the degree of Master of Science

in the

Faculty of Science and Technology
Department of Biology, Chemistry and Environmental Engineering

June 1, 2019

Declaration of Authorship

I, Charlotte Wiemann, declare that this thesis titled, "Development of a portable surface plasmon based genosensor for the detection of obligate hydrocarbon degrading bacteria in the marine environment" and the work presented in it are my own. I confirm that:

- This work was done wholly or mainly while in candidature for a research degree at this University.
- Where any part of this thesis has previously been submitted for a degree or any other qualification at this University or any other institution, this has been clearly stated.
- Where I have consulted the published work of others, this is always clearly attributed.
- Where I have quoted from the work of others, the source is always given. With the exception of such quotations, this thesis is entirely my own work.
- I have acknowledged all main sources of help.
- Where the thesis is based on work done by myself jointly with others, I have made clear exactly what was done by others and what I have contributed myself.

Signed: 

Date: 01.06.2019

UNIVERSITY OF STAVANGER

Abstract

Faculty of Science and Technology

Department of Biology, Chemistry and Environmental Engineering

Master of Science

by Charlotte Wiemann

This study aimed at developing a genosensor that could be implemented in the Environmental Sample Processor (ESP) based on surface plasmon resonance (SPR) to detect obligate hydrocarbonoclastic bacteria (OHCB) that can be used as bioindicator species for oil spill events in the marine environment. The final goal was to obtain an SPR assay for the selective and quantitative detection of the OHCB *Oleispira antarctica* within the context of whole microbial communities, employing a 16S rRNA capture technique for selective enrichment and signal amplification. A custom-made portable SPR instrument was used to develop the assay. The 16S rRNA from *O. antarctica* was extracted and different hybridization protocols and buffers were tested to selectively enrich the target 16S rRNA out of a pool of RNA. Only one procedure tested yielded promising results. RNA extraction with ESP buffer has proven to be comparable to commercially available extraction methods. Presence and size of the extracted products were verified with reverse transcriptase polymerase chain reaction (RevT-PCR). The SPR sensors surfaces were coated with morpholinos to specifically detect synthetic oligonucleotide sequences mimicking the 16S rRNA of *O. antarctica*. The morpholino-based DNA detection was characterized in terms of specificity by comparing mismatch oligo signals in different buffer conditions. The mismatched oligos could be differentiated from perfect match oligos at concentrations of 0.5 nM with all buffers yielding best results in DPBS. The sequential amplification approach has proven to excellently work for 45-nt oligonucleotides at concentrations of 0.5 nM. It was used to further detect longer molecules (i.e. 90 bp cDNA), resulting in very low signal intensities. This study has shown that it is possible to use ESP buffer for the extraction of RNA and to detect 45-nt long oligonucleotides in a concentration of 0.5 nm with the SPR instrument.

Acknowledgements

I am very grateful for the valuable guidance my supervisor Andrea Bagi gave me throughout the work on this thesis, for her patience and for taking the time to explain the details of this project more than once to me. Special thanks to my supervisor at the university, Daniela Pampanin, for her guidance throughout the project and who made it possible for me to work on this particular topic. I also want to thank José Antonio Torres for his valuable input and moral support. At last I want to thank my close friends and family for supporting me throughout this year, for their critical remarks and suggestions and for cheering me up when I needed it.

Contents

List of Figures

List of Tables

List of Abbreviations

ATR	**A**ttenuated **T**otal **R**eflection
AUV	**A**utonomous **U**nderwater **V**ehicle
bp	**B**ase **P**air
DAPI	4′,6-**di**a**m**idino-2-**p**heny**l**i**n**dole
ddPCR	**d**roplet **d**igital **P**olymerase **C**hain **R**eaction
DPBS	**D**ulbeccos' **P**osphat **B**uffered **S**aline
DPBS-T	DPBS with 0.1% Tween-20
DPBS-U	DPBS with 200 mM urea
DWH	**D**eep **W**ater **H**orizon
FISH	**F**luorescent **i**n-**s**itu **H**ybridization
FSC	**Forward Sc**atter
HBI	**H**ybridization **B**uffer with 25% formamide
HBII	**H**ybridization **B**uffer
HRP	**H**orse **R**addish **P**eroxidase
HBU	**H**ybridization **B**uffer with **U**rea
LNA	**L**ocked **N**ucleic **Acid**
LOC	**L**ab-**O**n-a-**C**hip
LOD	**L**imit **o**f **D**etection
LR-AUV	**L**ong-**R**ange **A**utonomous **U**nderwater **V**ehicle
mRNA	**m**essenger **RNA**
MPN	**M**ost **P**robable **N**umber
NASBA	**N**ucleic **A**cid **S**equence **B**ased **A**mplification
NGS	**N**ext **G**eneration **S**equencing
OD_{600}	**O**ptical **D**ensity at 600 nm
OHCB	**O**rgano **H**ydro**c**arbon degrading **B**acteria
PAH	**P**olycyclic **A**romatic **H**ydrocarbon
PCR	**P**olymerase **C**hain **R**eaction
PNA	**P**rotein **N**ucleic **Acid**
qPCR	**q**uantitative **P**olymerase **C**hain **R**eaction
RFLP	**R**estriction **F**ragment **L**ength **P**olymorphism
RIU	**R**efractive **I**ndex **U**nit
ROV	**R**emotely Operated **U**nderwater **V**ehicle
rRNA	**r**ibosomal **RNA**
RT	**R**oom **T**emperature
RevT	**Rev**erse **T**ranscription
RevT-qPCR	**Rev**erse **T**ranscriptase **q**uantitative **P**olymerase **C**hain **R**eaction
SHA	**S**andwich **H**ybridization **A**ssay
SPR	**S**urface **P**lasmon **R**esonance
SPRi	**S**urface **P**lasmon **R**esonance **i**maging
ss	**S**ingle **S**tranded
SSC	**S**aline-**S**odium **C**itrate
SC	**S**ide Sc**a**tter

SNP	**S**ingle **N**ucleotide **P**olymorphism
TIRF	**T**otal **I**nternal **R**eflection **F**luorescence
VNTR	**V**ariable **N**umber **T**andem **R**epeat
VOC	**V**olatile **O**rganic **C**ompound

List of Symbols

A	Absorbance	
c	velocity of light in vacuum	
d	length of cuvette	
n	refractive index	
v	velocity of light in medium	
ϵ	extinction coefficient	$M^{-1} \times cm^{-1}$
λ	wavelength	nm
Θ_c	critical angle	$^\circ$

1 Introduction

Oil polluting events, which can be caused by many incidents, can seriously affect the marine environment. Unintended release of oil into seawater during drilling processes, transportation or through leakages of pipelines and vessels, brings the need to investigate the degradation of oil especially in cold-marine environments. Traditional monitoring approaches fail to combine analysis with transmission of data and information of the decision makers about possible oil leakages. Especially in areas that are difficult to access, the continuity of monitoring is not always ensured, calling for next generation remote monitoring and autonomous samplers capable of doing so [38, 39, 41]. Over 90% of the seawater volume has temperatures below 4°C [24]. Obligate hydrocarbonoclastic bacteria (OHCB), present in seawater, have been found to react rapidly to contamination with oil or its constituents at these temperatures in the marine environment [92]. OHCB have a metabolism that is restricted to aliphatic hydrocarbons and their derivates [43]. Among the OHCB found most abundant in oil-polluted seawater was *Oleispira antarctica*, a geographically widespread bacterium [25, 40, 92]. Its concentration drastically increases when alkanes are present in the marine ecosystem [40, 91]. The high sensitivity of *O. antarctica* makes it a promising biosensor for the detection of marine oil contamination.

2 Background

2.1 Hydrocarbon pollution in the marine environment

The worldwide oil production was 11.0 million tons per day by the end of 2000. It increased over 30% within 16 years, from 8.5 million tons back in 1984 [61]. Oil spills represent one of the major challenges for the marine environment. Incidents like the Deep-Water Horizon (DWH) blow-out in 2010, Exxon Valdez (1989) or Prestige accident (2002) demonstrated the consequences of oil spills on the environment and the need to work towards solutions of remediation after those.

2.1.1 Sources

Hydrocarbons from crude oil can enter the marine environment in different ways. They naturally occur due to leakages from oil reservoirs, referred to as natural oil seeps, which make up approximately 47% of the worldwide petroleum hydrocarbon input into the sea [61]. However, the increased demand and consumption in crude oil over the last years led to an increase of production and transportation. Accidental discharges, for example in the forms of oil spills and atmospheric deposition of volatile organic compounds (VOC) from transportation (e.g. tanks and pipelines) or offshore platforms, enable the petroleum hydrocarbons to enter the marine environment [7]. These accidental discharges account for approximately 15% of the worldwide input, while the consumption of oil contributes to approximately 38% of the overall petroleum hydrocarbon input into the marine ecosystem [61].

2.1.2 Fate and effect

Crude oil can consist of more than 20 000 different compounds [52], which can be divided into four classes: 1) saturates, 2) asphaltenes, 3) aromatics, and 4) resins [31, 44]. Hydrocarbons are one of the most abundant components of crude oil [32]. They include polycyclic aromatic hydrcarbons (PAH) which are of high concern due their carcinogenic potential [61, 67]. The presence of oil in the marine environment, for instance through regular (produced water) or accidental discharges (such as spillages or leakages), has various harmful sublethal effects on the marine life [2, 14]. It may lead to acute or chronic effects such as physical and reproductive impairment, decline in growth or decrease of waterproofing and insulating properties in feathers of birds and pelage of mammals [55, 58, 61]. The natural removal of oil from the

environment is very slow and takes several years. Bioremediation has proven to be a possibility to respond to pollution events, yet its effectiveness and consequences are controversial, and it varies with the composition of the oil [31]. Different conditions like weathering, photochemical modification or evaporation have effects on the availability and stability of the oil and its constituents [55, 61]. The dispersion of oil results in the formation of droplets that increase the oils surface area and its diffusion into the water phase. This can be naturally achieved by the release of biosurfactants from microbial activity [44]. Chemical dispersants act in a similar manner by facilitating the oil dispersion process and natural biodegradation from bacterial species. Some of the oil-originated components can adsorb to organic material and other compounds, thus decreasing their bioavailability [55].

2.1.3 Current monitoring

Several strategies exist to monitor oil spills occurring in the sea, from small-scale infrared and ultraviolet line scanners, microwave radiometers and x-band radar systems to side-looking airborne radars (SLAR) and observation with satellites, so called space-acquired synthetic aperture radars (SAR). However, these methods are not suitable to measure small scale events occurring through leakages from pipelines, abandoned vessels or accidental discharges [21]. Currently, samples are still collected from the shore or through shipboard surveys and further on processed and analyzed in the laboratory [41]. However, automated measurements with instruments and platforms like remote-operated systems (ROV), autonomous underwater vehicles (AUV) or smart-buoys have been developed and deployed [38].

2.1.4 Monitoring needs and future perspectives

The increasing demand for fast and near-real time monitoring is leading to the development of more cost-efficient detection methods. The monitoring systems are supposed to be easy portable, yet being specific enough. Several approaches using mobile-phone based biosensors [28, 47, 73] have been published, allowing high connectivity meanwhile being very cost-efficient. To reduce costs, 3D printers have been employed. The use of paper-based biosensors has been reported as well [73]. Furthermore, Lab-on-a-Chip (LOC) as well as next-generation sequencing (NGS) approaches are promising tools for the detection of biomolecules [20, 57]. Low concentration or poor accessibility of the target demand methods for improvement of specificity and sensitivity. Hence, signal amplification methods, such as Nanobioengineered platforms, coated with nanomaterials like quantum dots, silver or gold nanoparticles to increase sensitivity [42, 57], polymerase chain reaction (PCR) or nucleic acid sequence-based amplification (NASBA) can be suggested [5]. Medlin et. al [57] reviewed several methods for the molecular detection of specific organisms, which can be for instance used as markers of pollution events in the marine environment.

2.2 Genosensing

2.2.1 Molecular based diagnostic tools in marine environmental monitoring

Several molecular methods exist to detect biomolecules in environmental samples. According to Medlin et. al [57], a way of dividing them is to distinguish between whole cell and cell-free methods. One of the most well-known whole cell methods is the fluorescence in-situ hybridization (FISH), where an oligonucleotide probe, coupled to a fluorescent marker, penetrates the cell and attaches to the ribosome [57]. This method is advantageous since cells can be visualized by fluorescent microscopy. Cell-free methods have a higher rRNA and DNA content compared to whole cell methods [3]. The two most commonly employed methods are the semi-quantitative microarrays and the quantitative polymerase chain reaction (qPCR). Microarrays are used for the detection of thousands of targets in one hybridization [57]. Specific probes are immobilized onto a surface in rows and columns. They are hybridized with their complementary target. The hybridization creates a signal that can be measured and further evaluated to identify the unknown target sample [26]. The Sandwich hybridization assay (SHA) is a widely used method and can also be applied on microarrays. A specific probe, complementary to the desired target, is immobilized on a surface. The binding of the target to the capture probe is followed by the hybridization of a signal probe to the target in order to amplify the signal. This signal probe is coupled to an amplification element. This can be, for instance, digoxigenin that can be detected through the addition of horseradish peroxidase (HRP). HRP converts it into a product which eventually can be detected either colorimetrically or electrochemically [57, 65]. Besides, qPCR is used for giving information about the quantity of the starting material. Using qPCR, one can distinguish base pair (bp) differences. DNA is logarithmycally amplified in a number of cycling events in real-time as the reaction proceeds to favor the detection of low abundant gene targets. For this purpose, a fluorescent marker is used and the fluorescence intensity is measured with proceeding amplification. The increasing fluorescence intensity is proportional to the increasing concentration of the product. The quantity can be determined through the usage of a prepared dilution series with known concentrations. The fluorescence intensities will be compared to the samples' fluorescence and thus the initial concentration can be determined. When RNA is the starting material, reverse transcriptase-qPCR (RevT-qPCR) can be applied, employing the enzyme reverse transcriptase that transcribes RNA into its complementary DNA.

2.2.2 The Environmental Sample Processor

The environmental sample processor (ESP), also referred to as "lab in a can", is a fully autonomous device for near real-time monitoring of water samples. It is commercially available from *McLane Research Laboratories* [68] and can be used for operations in the deep sea ($\leq$ 1000 m, [77]). The 2^{nd} generation ESP (2G ESP) is used in the field. However, due to its size and limited mobility a more compact 3^{rd} generation ESP (3G ESP) is under development [60]. The 2G ESP consists of small chambers, referred to as "pucks", with a filter, through which water is pulled to collect sampling material. The system employs DNA and protein probe arrays for the target detection [40]. Samples can either be preserved and archived through addition of preservatives to the filter or they can be further processed *in situ*. The DNA array utilizes a SHA and qPCR, while the protein array employs a competitive enzyme-linked immunosorbent assay (ELISA) [9, 77]. The 3G ESP is fully integrated on a long-range AUV (LR-AUV) [60], together with several modules such as surface plasmon resonance (SPR), whilst digital droplet PCR (ddPCR) and total internal reflection (TIRF) are under development. The SPR system that has been used in this study has the same working principle and functions as the miniaturized one currently used on the 3G ESP [6].

2.2.3 Surface plasmon resonance based genosensing

SPR is a technology for label-free and near real-time detection of biomolecules. It measures changes in the relative refractive indexes on a metal-dielectric interface. These changes occur through absorption of p-polarized light by surface electrons on the metal film [27, 35].

Theoretical background

Electromagnetic radiation is the propagation of orthogonal oscillating magnetic and electric fields perpendicular to the direction of motion and leads to the formation of a transverse wave [54]. In most SPR systems the Kretschmann geometry is used [76, 82, 83], where a metal film is placed on an interface consisting of two media with different refractive indexes n. n is a dimensionless number that defines how fast light can transverse a medium and is described as

$$n = \frac{c}{v} \tag{2.1}$$

c: velocity of light in vacuum
v: velocity of light in the medium

If the incident radiation interacts with the interface, the free mobile electrons on the metal can correspond to it with almost no scattering [76]. When the incident radiation falls upon the interface with an angle Θ, two important possibilities arise:

the electric field vector can be parallel to the plane of incidence, referred to as p-polarized radiation, or perpendicular to it, referred to as s-polarized radiation [11, 76]. p-polarized radiation causes polarization charges at the interface, while s-polarized radiation normally won't result in any change of charges [76]. Depending on the discontinuity of the dielectric constant, the incident radiation will be reflected at a specific angle given by λ_2 defined by the equation

$$\lambda_2 = \frac{\lambda}{n_2} \tag{2.2}$$

λ: wavelength
n_2: refractive index of medium 2

When the incident radiation exceeds the critical angle Θ_c given by

$$\sin(\Theta_c) = \frac{n_2}{n_1} \tag{2.3}$$

n_1: refractive index of medium 1
n_2: refractive index of medium 2

the propagating wave cannot proceed in medium 2 and is totally reflected [83]. Due to the oscillating electric field, charges in medium 1 will start to oscillate and their associated radiation field will penetrate medium 2 [76, 83]. This results in the formation of evanescent waves in the lower refractive index medium 2 and excitation of the surface plasmons at the surface of the metal [82, 83], thereby leading to a minimum in the reflection coefficient referred to as attenuated total reflection (ATR) [89]. Binding or adsorption events on medium 2 change its refractive index and thus the resonance angle.
The SPR sensors employ immobilized detection probes on their surface for capturing the target molecules through affinity interaction [82]. Hence, binding events can be monitored in real-time [79]. The specificity and sensitivity of the SPR sensors depend on different factors, such as probe and sensor preparation, buffer composition, temperature, and pH values. The level of detection (LOD), which is defined as three times the standard deviation of the background signal, is highly dependent on those factors. According to Sipova [82], chemical solutions containing denaturants (e.g. formamide or urea), low salt concentrations (NaCl content below 300 mM) and high-ionic strength buffers (NaCl content over 300 mM or $MgCl_2$ content around 15 mM) can achieve lower LODs. The employment of thiolated probes and the use of streptavidin-biotin interaction in the immobilization approaches for achieving low LODs yielded similar results [82].

Instruments

Different SPR instruments can be found in the market. Among the most used commercially available laboratory instruments one can find the Biacore (Uppsalla, Sweden), IBIS' MX96 SPR imager (IBIS Technologies) and Reichert 4SPR (ATG Scientific, UK) instruments. However, these instruments cannot be applied in field analysis due to their size. Several portable instruments like the β-SPR system (Sensia, Spain) and Spreeta (Texas Instruments, USA) have been manufactured and used to serve these needs. Trends are going towards even smaller and lighter alternatives employing mobile phone-based SPR [47]. The portable SPR instrument used in this study was developed at the University of Washington (Seattle, WA, USA) and houses 4 SPREETA sensors with 3 channels each. The SPREETA sensors consist of a light source, a gold surface and a reflecting mirror on which the light is reflected towards a photodiode array (fig. 2.1).

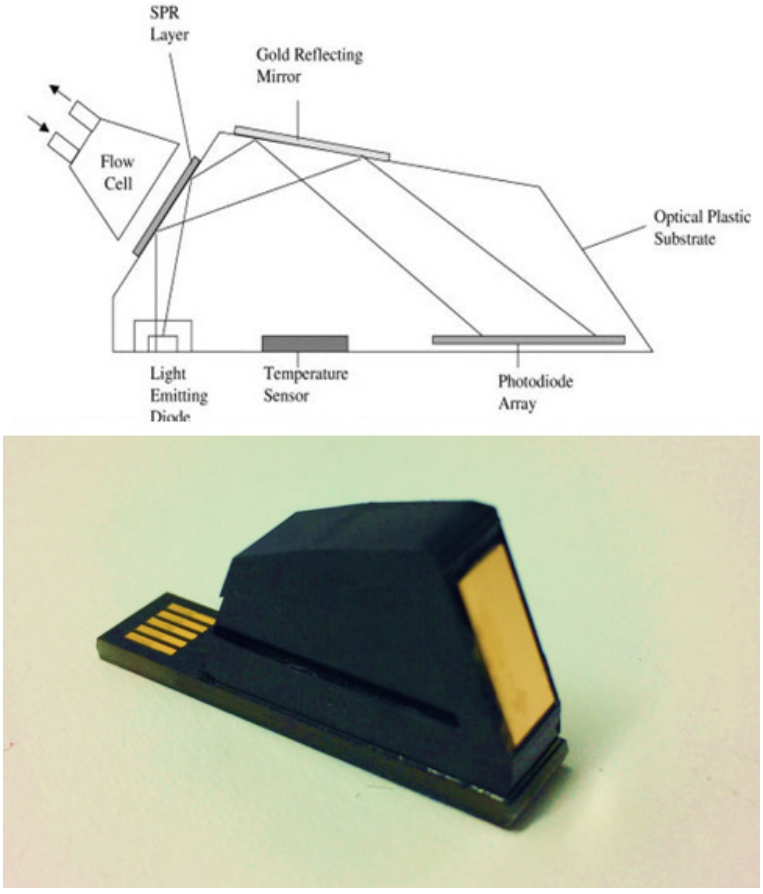

Figure 2.1: Optical diagram of the SPR sensor [19] and photo of a SPREETA sensor chip used in this study.

This instrument consists of a miniature peristaltic and a vacuum pump, as well as a temperature control. The system runs semi-autonomously, following a pre-set program. A "start" signal is required and the sample has to be injected by hand. Eventually, a regeneration solution is flushed to regenerate the sensors followed by

a running buffer to prepare the system for the next injection. The output signal is transferred to a digital signal, displayed as SPR curves where the refractive index unit (RIU) is plotted against time.

2.2.4 Recognition elements for genosensing

Genosensors are biosensors that employ nucleic acids to detect biological events [51]. Biosensors are devices containing biological sensing elements that are associated with a physicochemical transducer [66]. They are promising tools due to their cost efficiency, easy manufactoring [57], their possibility for integration in autonomous devices and their ability to measure pollutants with minimal sample preparation [66]. Biosensors that combine SHA and nucleic acid target molecules are among the most successful [57]. Nucleic acid biosensors are especially used in environmental monitoring [5]. They employ an immobilized probe composed of oligonucleotides with known sequence on the sensors' surface [5, 66]. The binding of a specific target nucleic acid to the probe causes changes in the characteristics of the sensing layer and thus can be detected. Different sensing elements like natural RNA or DNA sequences can be used for recognition. Other approaches employ artificial nucleic acids like peptide nucleic acids (PNA) [80], locked nucleic acids (LNA) [87] or morpholinos [45].
The detection of oligonucleotides is challenging due to their small size leading to an insufficient binding to surfaces [93]. In the recent years, SPR based biosensors have become a widely used tool for real-time, label-free and non-invasive monitoring of a variety of analytes [28, 82, 83, 95]. However, their performance is still dependent on a variety of factors such as hybridization conditions, sensor surface, sample composition and amplification methods [82].

Morpholino probes

Morpholinos are nucleic acid analogues that have several advantages over natural nucleic acids like RNA or DNA. They are composed of morpholino rings attached to phosphorodiamidates and nucleic acid bases (fig. 2.2) and comprise the natural ribonucleosides rA, rC, rC and the synthetic ribonucleoside rT [36].

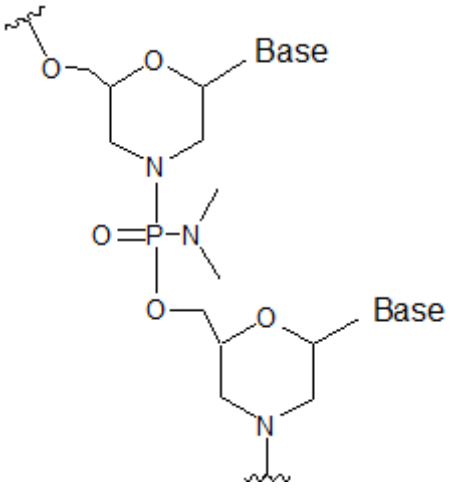

Figure 2.2: Morpholino structure.

Morpholinos are resistant to enzymatic degradation, have low toxicity *in vivo*, are highly affine to complementary DNA and are less dependent on the ionic strength of the medium due to their charge-neutral nature [36, 45]. Morpholinos have been used as recognition elements on the SPR sensor surfaces in this study.

2.3 Obligate hydrocarbon degrading bacteria

Many marine microorganisms, capable of using petroleum hydrocarbons as a carbon source, have been isolated [55]. Some of them use hydrocarbons as their sole growth substrate [31]. These so called obligate hydrocarbonoclastic bacteria (OHCB) play an important role in the removal of crude oil from the marine environment [91]. Within these, the genera of gammaproteobacteria, which mainly consist of aerobe bacteria [84], is among the most abundant [56], including bacteria of the genera *Oleispira, Oleiphilus, Marinobacter, Alcanivorax, Thalassolituus* and *Cycloclasticus* [13, 91]. The metabolism of OHCB is restricted to a few compounds resulting in a very specialized substrate specificity [91]. The substrate preferences differ among the genera, for instance *Oleispira* and *Oleiphilus* grow on aliphatic hydrocarbons while *Cycloclasticus'* growth is limited to aromatic hydrocarbons [31].

2.3.1 Microbial response to oil in the sea

Microbial community changes

Microorganisms are naturally exposed to hydrocarbon sources from crude oil through natural seeps. This led to the evolution of marine organisms capable of using petroleum-originated hydrocarbons as their main carbon source [55]. The biodegradation of petroleum is influenced by many factors and is highly dependent on its composition. The solubility is temperature dependent resulting in different availability of

the compounds with changing temperature. Furthermore, the petroleum's composition, as well as nitrogen and phosphorus content in the seawater play an important role [29, 55]. Supplementation of polluted environments with phosphorus and nitrogen has proven to support bioremediation [31, 91]. Dispersants are often employed to break up the oil into smaller droplets. The biodegradtion rates increase with decreasing droplet size due to their higher surface-size ratio [12]. Different conditions result in varying microbial response in the seawater after the exposure to oil. However, there are some common trends: Alpha- and gammaproteobacteria have been found to dominate after enrichment with oil [16]. The bacteria *Alcanivorax borkumensis* [30, 31], capable of degrading alkanes, *Cycloclasticus*, capable of degrading PAHs [55] and *O. antarctica* [40, 91], among other bacteria like *Acinetobacter, Thalassolituus*, and *Pseudoalteromonas*, increase drastically in concentration after enrichment with oil. *O. antarctica* has been found to become abundant in cold marine environments [91] and to dominate the microbial community at cold temperatures around 4°C [16].

Microbial gene expression

OHCB evolved very efficient systems to degrade hydrocarbons, normally producing surfactants or optimizing their access to oil through hydrophobic outer envelopes [74, 78]. The aerobe degradation of medium length alkanes is initiated by alkane hydroxylases [32]. The degradation starts with oxidizing the terminal methyl-group [74]. Some bacterial strains contain alkane monooxygenases closely related to *AlkB* alkane hydroxylase, while other comprise enzymes belonging to the family of cytochrome p450 [74]. *AlkB* employs rubredoxin and rubredoxin reductase as main electron transfer components that are needed for alkane hydroxylation [32, 64]. *AlkB* and *CYP153* have been simultaneously detected in *Marinobacter, Alcanivorax, Rhodococcus* and *Mycobacterium* [64].

2.3.2 Molecular markers of OHCB

Phylogenetic markers

To characterize the taxonomy of bacteria one can use phylogenetic markers such as 16S rRNA, or fragments of other nucleic acids or proteins [18]. Prokaryotic ribosomes consist of two subunits, a small 30S and a large 50S subunit, which together form the 70S ribosome. The large subunit consists of two kinds of ribosomal RNA (rRNA), the 5S and 23S rRNA, while the small subunit consists of the 16S rRNA. Its high conservation among the different species of bacteria makes the 16S rRNA suitable for the use for phylogenetic studies [15]. It is advantageous due to being present in almost all bacteria and with around 1500 bp being large enough to serve for informational purposes [37]. In bacteria, RNA expression levels correlate with microbial activity and high copy number of 16S rRNA [22]. The Phylochip is a commercially available 16S rRNA targeted microarray with 500 000 oligonucleotide probes to identify bacteria and archea [57, 62]. It enables fast detection of microorganisms in

complex environmental samples. Microarrays are advantageous compared to other molecular detection techniques due to their rapid and low detection limit [20].

Functional markers

Functional markers are used to control whether a certain metabolic process is present in an organism by targeting the messenger RNA (mRNA) or genes encoding it. The presence or absence of the genes encoding for a specific metabolic process give information about its occurrence. Among the most commonly used are restriction fragment length polymorphism (RFLP), single nucleotide polymorphism (SNP) and variable number tandem repeat (VNTR). The GeoChip is a functional gene DNA microarray with genes that are involved in biogeochemical processes like the nitrogen, carbon, sulfur or phosphorus cycling [34]. It is a promising tool for the detection of microbial populations. It contains more than 24 000 genes [34] and can simultaneously detect microbial populations and functional groups within microbial communities [90]. Various genes are known to be involved in the degradation of petroleum hydrocarbons, such as *alkB*, *alkM* (alkane monooxygenases), *xylE* (catechol dioxygenase) and *nahAc* (naphthalene dioxygenase) [1, 49, 88]. Their presence and abundance can be used as an indicator to predict whether the analyzed species are able to degrade hydrocarbons [48].

2.3.3 Oleispira antarctica

The bacterium *O. antarctica RB-8* belongs to the genus *Oleispira* and is a marine OHCB. Its 16S rRNA was found predominant after the DWH blow-out in 2010 [33, 53]. *O. antarctica* was first isolated in 2000 from crude-oil enrichments in Antarctic seawater [92] and is found predominantly in cold-marine environments [16, 25]. Its cells are helical shaped and between 2 to 5 μm in length [92]. Being a psychrophilic bacterium, it has an optimal growth temperature between 1 and 15°C [24, 92]. Most of its proteins show characteristics of cold-adapted enzymes having an increased surface hydrophobicity and surface negative charges as well as less total charged residues [43]. It grows poorly on acetate and pyruvate while volatile fatty acids, Tween and aliphatic hydrocarbons support it [24, 92]. As a marine organism it needs NaCl for growth [92]. The genome analysis of *O. antarctica* revealed the presence of three genes for alkane monooxygenases and fatty acid desaturases, so far the largest number found in gammaproteobacteria [43]. Alkane oxidation (terminal) is initiated by monooxygenases, yielding alcohols as intermediates, which are converted to aldehydes and fatty acids by alcohol and aldehyde dehydrogenases [75].

Cultivation of Oleispira

For the cultivation of *O. antarctica* a medium mimicking sea conditions is required. The ONR7a medium is a high saline medium and can be supplied with carbon sources like Tween-40, sodium-pyruvate or tetradecane to ensure *O. antarcticas'* growth.

The bacteria grow well on Marine Broth 2216 (Difco) at temperatures ranging from 4 to 20°C [92].

Methods for tracking the Oleispira culture

Bacterial cultures can be tracked with different methods depending on the research needs. The growth of cultures can generally be observed with spectrophotometry, a method that measures the absorbance of light sent through a sample. The denser the culture, i.e. the more cells in the sample, the more light is absorbed yielding a higher absorbance. This phenomenon can be expressed with the Lambert-Beer-law:

$$A = \epsilon \times c \times d \tag{2.4}$$

A: Absorbance
ϵ: extinction coefficient
c: concentration
d: length of the cuvette

Since ϵ and d are held constant throughout the measurements, the absorbance is directly proportional to the concentration.
For the determination of the total number of bacteria one can use the dye 4,6-diaminidino, 2-phenylindole (DAPI) cell counting method, which is relatively very fast. It is specific towards DNA and fluoresces blue when excited at a wavelength of 365 nm and in a complex with DNA [70]. Its unbound counterpart will fluoresce yellow.
For counting cell numbers one can also use flow cytometry. Here the scattering of light, caused by samples that pass through a laser beam, is measured. Typically, the forward (FSC) and side (SC) scattering of the light is measured. The FSC gives information about the size of the particle while the SC gives information about the granularity or internal strucutre of the cell [50]. Bacterial cells in this experiment are stained with SYTO9, a green-fluorescent dye that is highly specific towards DNA and can be excited by the lasers. In order to exclude signals that are due to background noise or generally unwanted, a threshold has to be set. The threshold is the lowest signal intensity at which an event will be recorded [10].
The most probable number method is used to estimate the concentration of cultivatable microorganisms in a sample [81]. The microorganisms' growth is observed in 10-fold serial dilutions. Tubes, filled with liquid-broth, will turn turbid when growth occurs. In the original approach, 1 part of homogenate is added to 9 parts uninoculated enrichment, proceeding until reaching a 10^{-10} dilution with the same ratio of homogenate to broth [4]. The samples are incubated in triplicates. Tubes might not be inoculated with any cells as the dilution increases. Growth in the tubes is compared to a given table (for instance US Food and Drug Administration: Bacterial Analytical Manual (BAM) [8]) in order to obtain the most probable numbers [81].

2.4 Objectives

The aim of this method development was to work towards establishing a protocol for SPR analysis to be integrated in the 3G ESP, to specifically and quantitatively detect *O. antarctica* in whole microbial communities. For that a 16S rRNA capture technique for enrichment and amplification was employed.

In order o achieve this goal, the aim was to characterize the morpholino based DNA detection in terms of its specificity by investigating the effect of different buffer conditions (DPBS, DPBS with 0.1% Tween, DPBS with high or low salt content, DPBS with urea) on mismatch oligo signals.
It was worked towards the development of a protocol for fast RNA treatment of environmental samples to selectively enrich target 16S rRNA from an RNA pool, working with 1500 bp long molecules with secondary structures. Different hybridization protocols and buffers were tested in terms of capture efficiency to capture the target 16S rRNA.
Furthermore, this study aimed for determining rRNA detection limits using *O. antarctica* rRNA. Plate counting, flow cytometry and a modified version of the most probable number method were employed for establishing the minimum number of *O. antarctica* cells that the used SPR system was able to detect. In order to test the ability of the SPR instrument to detect longer molecules, PCR products were generated from 90 and 477 bp long gene fragments and a sequential amplification approach performed on the instrument.

3 Materials and Methods

3.1 Oleispira cultivation

Media

O. antarctica was obtained from DSZM as live culture and maintained in the laboratory as culture in liquid Marine Broth Medium (MBM DSM 514) amended with Tween-40 as Oleispira-specific carbon source. MBM DSM 514 (100 mL) was inoculated with 1 mL Oleispira culture and incubated in the dark on a shaker. Solid marine agar was only used for plate counting.

Preparation of media

The Marine Broth Medium (MBM DSM 514) was used for the cultivation of *O. antarctica* and was supplied with 1% Tween-40. The medium was prepared in 1 L Milli-Q water respectively.
The MBM contains: Bacto peptone (5.00 g/L), Bacto yeast extract (1.00 g/L), Fe(III) citrate (0.10 g/L), NaCl (19.45 g/L), $MgCl_2$ (anhydrous, 5.90 g/L), Na_2SO_4 (3.24 g/L), $CaCl_2$ (1.80 g/L), KCl (0.55 g/L), $NaHCO_3$ (0.16 g/L), KBr (0.08 g/L), $SrCl_2$ (34.00 mg/L), H_3BO_3 (22.00 mg/L), Na-silicate (4.00 mg/L), NaF (2.40 mg/L), $(NH_4)NO_3$ (1.60 mg/L), Na_2HPO_4 (8.00 mg/L).
The ingredients were dissolved in Milli-Q water under heating and vigorous stirring until the mixture became clear. The solutions were autoclaved at 121°C for 20 min and Tween-40 added to the still warm mixture. Then, the mixture was filter-sterilized (0.22 μm).
The Marine Agar 2216 (MA2216, Difco) was supplied with 1% sodium-pyruvate and prepared in 1 L Milli-Q water.
The MA2216 contains: Peptone (5.00 g/L), Yeast extract (1.0 g/L), Fe(III) citrate (0.1 g/L), NaCl (19.45 g/L), $MgCl_2$ (8.8 g/L), Na_2SO_4 (3.24 g/L), $CaCl_2$ (1.8 g/L), KCl (0.55 g/L), $NaHCO_3$ (0.16 g/L), KBr (0.08 g/L), $SrCl_2$ (34.0 mg/L), H_3BO_3 (22.0 mg/L), Na-silicate (4.0 mg/L), NaF (2.4 mg/L), $(NH_4)NO_3$ (1.6 mg/L), Na_2HPO_4 (8.0 mg/L), agar (15.0 g/L).
As described for the MBM DSM 514, ingredients were dissolved in Milli-Q water, gently heated up and stirred until the mixture became clear. Sodium-pyruvate was added before autoclaving the solution at 121°C for 20 min. The agar solution was allowed to cool down to 60°C before pouring it on the plates.

Maintenance of the liquid culture

One *O. antarctica* culture was maintained continuously at 10 to 12°C, while for an experiment to compare growth characteristics, a culture at 4°C was also set-up. The cultures were incubated in the dark on a shaker at 4 and 12°C respectively. The optical density at 600 nm (OD_{600}) was measured daily. A blank, only containing medium (MBM DSM 514), was measured as well and the mean average of its values subtracted from the obtained values of the Oleispira cultures. All measurements were taken in triplicates.

Fluorescence microscopy (DAPI)

In order to confirm the presence of *O. antarctica* in the cultures, cells were stained and observed under a fluorescence microscope (Axioplan2 imaging). The stock solution of the DAPI stain (Invitrogen, 1 mg/mL) was 10x diluted prior to use. The *O. antarctica* culture (45 μL) and 5 μL stain were combined in a tube and incubated for 10 min in the dark. Water (950 μL) was added to the tube and the mixture was vacuum-filtered (0.22 μm). The filter containing the cells was placed on a microscope slide containing one drop of antifade mountant and covered with a glass slip.

3.2 Quantification of Oleispira

Spectrophotometry was used in order to obtain the ideal point in time to extract RNA from *O. antarctica* cells and in order to obtain growth curves. The most probable number method was used to estimate the order of magnitude of cells in the liquid culture, while plate counting and flow cytometry were employed to obtain total cell numbers. The obtained cell numbers from the latter two methods were used to estimate the total RNA content of Oleispira cells through extraction and quantification experiments on the same culture.

Spectrophotometry

The OD_{600} was measured with a spectrophotometer (MultiscanGo, Thermo Scientific). Each sample was pipetted onto a 96-well plate (200 μL) and OD measured at 600 nm after 15 s of agitation at high speed. All measurements were taken in triplicates. A blank was included and subtracted from obtained values.

Most probable number (MPN)

A modified version of this method was used in order to estimate cell numbers based on the dilution to extinction technique.
Fifty mL of DSM 514 medium were inoculated with 1 mL of an *O. antarctica* culture and incubated in the dark at 10°C for four days until the exponential phase was reached. A dilution series was prepared by adding 1 mL of the culture to 9 mL DSM

514 medium in a 15 mL test tube (concentration of 10^{-1}). One mL of the well mixed 10^{-1} culture was taken and added to 9 mL medium to achieve a 10^{-2} diluted culture. This process was repeated until reaching a dilution of 10^{-10} of the original culture (fig. 3.1). The test tubes were incubated on a shaker in the dark at 10°C and their growth observed through spectrophotometry (OD_{600}).

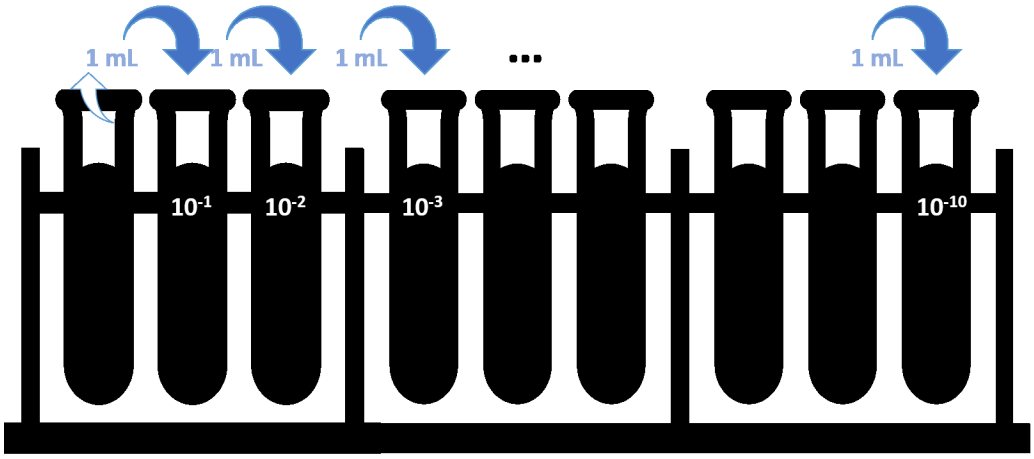

Figure 3.1: Schema of the preparation of the serial dilution for the most probable number approach.

Plate counting

For determination of the initial concentration of the Oleispira culture a dilution series was prepared down to a dilution of 10^{-10}. From the 10^{-4} to 10^{-10} cultures, 100 μL were taken and plated on MA2216 plates. All cultures were plated in triplicates and incubated in the dark at 10°C. The growth of colonies was observed daily. Occurring colonies were marked and counted after 5 days of incubation.

Flow cytometry

One mL of cells from an Oleispira culture was pelleted, washed twice with filtered seawater (FSW) and resuspended in 1 mL FSW. The sample (500 μL) was incubated with 125 μL SYTO9 (5 μM in Tris-EDTA) for 15 min in the dark. The cells of the stained and unstained 10^{-2} to 10^{-4} dilutions were counted in triplicates with a flow cytometer (BD Accuri, C6 Flow Cytometer). A blank, only containing FSW (stained and unstained), was measured and the obtained number subtracted from the samples' values. Per measurement, 50 μL of sample were analyzed. The threshold needed to be set to fluorescence rather than size in order to distinguish bacterial cells from background which occured to have particles of the same size. The threshold was set to FL1-H 750. FL1 is the detector for green light, emitted from samples upon staining with a fluorescent dye. Setting the threshold to FL1-H 750 means, that only

events with FL1 values above 750 will be recorded, using the height measurement (H) [10].

Estimation of RNA content per cell

In order to obtain the total RNA content per cell, dilution series were plated on MA2216 plates as briefly described above. Dilutions from 10^{-4} to 10^{-7} were plated in triplicates and incubated in the dark at 10°C for 5 days. The obtained number of colonies was used to calculate the amount of RNA per cell.

3.3 RNA extraction

A commercially available kit for RNA extraction was used in order to obtain the total RNA material for the RNA capture experiments. In addition, an ESP compatible cell lysis method was tested and compared to the performance of the commercially available method. Furthermore, another commercially available kit was used to simultaneously extract DNA and RNA from an Oleispira culture in order to estimate cell numbers based on the amount of extracted DNA and to calculate the RNA content per cell. Prior to extraction, the OD_{600} was recorded and cells were harvested through centrifugation (8 000 rpm, 10 min, 4°C). The obtained pellets were processed immediately or stored at -80°C until further usage. The RNA was extracted from Oleispira cultures in their exponential phase ($OD_{600} \geq 0.9$). For the estimation of RNA content per cell, RNA was extracted from *O. antartica* cells and the cells were counted using flow cytometry.

3.3.1 Commercially available method

PureLink

Following the protocol of *Pure link RNA mini kit* (Invitrogen), using the lysozyme buffer option, RNA was extracted from *O. antarctica* cells.

Pellets of *O. antarctica* were thawed on ice. A lysozyme solution was freshly prepared. It contained 10 mM Tris-HCl, 0.1 mM EDTA and 1 mg lysozyme per sample. The pellet was resuspended in 100 μL fresh lysozyme solution, vortexed and incubated at 37°C for 10 min. From a 10% SDS-solution 0.5 μL was added to the mixture and vortexed, followed by 5 min incubation at room temperature (RT, 21°C). Lysis buffer, provided by the kit, was prepared with 1% 2-mercaptoethanol and 350 μL of it added to the mixture. The preparation was vortexed and centrifuged (12 000 rcf, 2 min, RT). The supernatant was pipetted into a fresh RNase-free tube and 250 μL 100% ethanol was added and the mixture vortexed. The mixture was transferred into a spin cartridge (in a collection tube) and centrifuged for 15 s at 12 000 rcf at RT, the flow-through was discarded.
An on-column DNase treatment was included to remove contaminating DNA. For

that, a DNase cocktail (tab. 3.1) was prepared for the number of samples used and kept on ice until needed.

Table 3.1: DNase cocktail per sample for Pure Link RNA extraction and DNase on-column treatment.

10X DNase I Reaction buffer (digestion buffer)	8 μL
Resuspended Dnase	10 μL
RNase-free water	62 μL

Wash buffer 1 (350 μL) was added, centrifuged at 12 000 g for 15 s and flow-through and collection tube discarded. The cartridge was inserted into a fresh collection tube and 80 μL DNase cocktail (tab. 3.1) added to the surface of the membrane. The cartridge was incubated for 15 min at RT. Wash buffer 1 (350 μL) was added, centrifuged and the flow-through discarded. After that, 500 μL Wash buffer 2 was added, centrifuged (12 000 rcf, 15 s, RT) and the flow-through discarded. This step was repeated once. The cartridge was centrifuged for 1 min at 12 000 rcf, the collection tube discarded and the spin cartridge transferred into a recovery tube. The RNA was eluted in 50 μL DNase-/RNase-free water which was given to the spin-cartridge, incubated for 5 min at RT and then centrifuged (15 000 rcf, 2 min, RT). The flow-through was kept for further experiments.

Zymo BIOMICS

Following the protocol of the *ZymoBIOMICS DNA/RNA Miniprep Kit* (Zymo Research) for on-column DNase treatment, RNA and DNA were extracted from *O. antarctica* cells.

Pelleted *O. antarctica* cells were resuspended in 750 μL DNA/RNA Shield and transferred into a bashing bead tube. The mixture was homogenized for 20 min (VortexGenie) at maximum speed and further spinned down for 1 min. A DNase I Solution for each sample was prepared, containing 5 μL DNase I in 75 μL DNA Digestion Buffer. The supernatant (400 μL at a time) was transferred into a fresh 1.5 mL eppendorf tube. One volume of DNA/RNA Lysis Buffer was added and mixed well, and the preparation transferred into a Spin-Away Filter. The mix was centrifuged at 10 000 rcf for 30 s and the filter, containing DNA, transferred into a new collection tube. On-column DNase treatment was included in this protocol. One volume of 100% ethanol was added to the flow-through and mixed well. The sample was loaded on a Zymo-Spin III CG column and centrifuged (10 000 rcf, 30 s). The column was washed with 400 μL DNA/RNA Wash Buffer and centrifuged (10 000 rcf, 30 s), whereupon 80 μL of the prepared DNase I Reaction mix were given directly onto the column matrix and incubated for 15 min at RT (21°C). After the incubation, 400 μL DNA/RNA Prep Buffer were added to the column and the sample centrifugated (10

000 rcf, 30 s). DNA/RNA Wash Buffer (700 μL) was added, centrifuged and further 400 μL DNA/RNA Wash Buffer added and the mixture centrifuged for 2 min. The column was transferred into a fresh eppendorf tube and 100 μL DNase/RNase-free water added to the column. The sample was incubated for 5 min at RT and centrifuged for 2 min at 12 000 rcf. A Zymo-Spin III HRC Filter was prepared through addition of 600 μL ZymoBIOMICS HRC Pre Solution, followed by a 3 min centrifugation step at 8 000 rcf. The eluted RNA was transferred into a prepared Zymo-Spin III HRC Filter (in a fresh eppendorf tube). The mix was centrifuged for 3 min at 16 000 rcf.

3.3.2 ESP-compatible method

Following the ESP extraction protocol, RNA was extracted from *O. antarctica* cells.

Pelleted *O. antarctica* cells were resuspended in 500 μL of ESP lysis buffer (15 mM EDTA, 50 mM Tris-Cl, 0.2% SDS, 2% sarkozyl, 3 M GuSCN) and incubated for 5 min at 85°C, while mixing occasionally. The lysate was filtered through a 0.22 μm syringe filter. For the clean-up of the samples the instructions of the *Zymo RNA Clean and Concentrator^{TM}-5* kit were followed: two volumes of binding buffer were added to the mixture, followed by 1 volume (of the entire mixture) of 100% ethanol. The mixture was transferred into a Zymo Spin IC column with a collection tube and centrifuged at 12 000 rcf for 1 min at RT. The flow-through was discarded. To remove contaminating DNA, the mixture had to be DNase treated. A DNase cocktail (tab. 3.2) was prepared for the number of samples and kept on ice until further usage.

Table 3.2: DNase cocktail per sample for ESP RNA extraction and DNase on-column treatment.

RNase-free DNase I	3 μL
10X reaction buffer	3 μL
RNA wash buffer	24 μL

RNA wash buffer (400 μL) was added to the mixture, centrifuged at 12 000 rcf for 1 min at RT and the flow-through discarded. The DNase cocktail (30 μL) was given to the surface of the column and incubated for 30 min at 37°C. The column was centrifuged at 12 000 rcf for 30 s and the flow-through discarded. To elute the RNA, 400 μL RNA prep buffer were added to the column, centrifuged at 12 000 rcf for 1 min and the flow-through discarded. Wash buffer (800 μL) was added, the mixture centrifuged at 12 000 rcf for 30 s and the flow-through discarded. This step was repeated with 400 μL RNA Wash buffer. The mixture was centrifuged at 12 000 rcf for 2 min, the flow-through discarded and the column transferred into a RNase-free tube. DNase-/RNase-free water (50 μL) was added to the spin-cartridge, incubated

for 5 min at RT and then centrifuged (10 000 rcf, 30 s, RT). The flow-through was kept for further experiments.

3.3.3 Quality control and quantification

To determine the concentration of the extracted RNA, Nanodrop analysis was performed (NanoDrop ND-1000). The quality of the extraction was controlled with gel electrophoresis (PowerPac^{TM} Basic, BioRad) on an 1.5% agarose gel. For the preparation of the 1.5% Agarose gel, 0.75 g of agarose were dissolved in 50 mL 1x TAE-buffer (40 mM Tris, 20 mM acetic acid, 1 mM EDTA). The mixture was gently heated in the microwave. To the warm mixture 5 μL of 10 000x Gel green (in DSMO) was added before casting it onto the gel mold. The gel was run for 60 min at 80 V with sample volumes of 5 μL. A molecular Imager (GelDoc^{TM}, XR+ Imaging System) was used for visualization of the gel.

3.4 Verifying the presence of target 16S rRNA fragment

The ESP lysis protocol might have fragmented the RNA, making it almost impossible to detect the target RNA. To verify whether the 477 bp fragment was still detectable out of the RNA pool extracted following the ESP protocol, the extract was reverse transcribed and further amplified. RNA extracted with the *PureLink RNA mini kit* was used as positive control. The quality of the resulting products was confirmed with gel electrophoresis.

Reverse transcription

A reverse transcription (RevT) Mastermix (tab. 3.3) was prepared for the number of samples used and kept on ice until use.

Table 3.3: Reverse transcription master mix for 1 sample (20 μL reaction).

molecular graded water	3.6 μL
10X RevT buffer	2 μL
25 mM $MgCl_2$	1.4 μL
10 mM dNTP mix	4 μL
100 mM DTT	1 μL
RNase inhibitor	1 μL
Multiscribe enzyme	1 μL

The DNase-treated RNA samples (5 μL of 50 ng/μL) were mixed with 1 μL of random hexamer primers in 200 μL PCR tubes and incubated at 65°C for 5 min followed by a 2 min incubation at 4°C. For the no template control (RevT-NTC), molecular

graded water was used instead of RNA. Of the RevT master mix 14 μL was added to the denatured RNA primer mix and incubated in the thermocycler at the following temperatures: 25°C for 10 min, 37°C for 30 min and 95°C for 5 min. The samples were kept at 4°C until further processing.

Amplification of cDNA

The resulting cDNA fragments were used as template in a subsequent PCR. The replicate RevT reactions were pooled and 2 μL pooled cDNA from each sample used as template. The samples were mixed with 23 μL freshly prepared mastermix. Its composition is outlined in table 3.4

Table 3.4: PCR master mix for 1 sample (23 μL reaction).

molecular graded water	5.5 μL
10 μM forward primer (Oleispira oligo)	2.5 μL
10 μM reverse primer (Universal probe)	2.5 μL
Platinum Hot Start 2X master mix	12.5 μL

The sequences for the primers used are outlined in tab. 3.5.

Table 3.5: Sequences of primers used for reverse transcription PCR.

Primer	**Sequence (5′-3′)**
Oleispira oligo	CTAGCTAATCTCACTCAGGCTCAT
Universal probe	TGTAGCGGTGAAATGCGTAGA

Positive and negative controls were included. The positive control contained 2 μL of 10x diluted DNA from *O. antarctica*. RNA and DNA of the organism *OLN3*, an oil-degrading marine microorganism isolated in house and shown to belong to the family *Alcanivoraceae* (results not shown), a no-template control (NTC) for either extraction before and after DNase treatment, a NTC for the reverse transcription (no enzyme) and a NTC for the PCR (containing 2 μL of water instead of template) were used as negative controls. The thermocycler for the PCR run was set according to the *Platinum HotStart* protocol:

94°C	2 min	
94°C	30 s	
60°C	30 s	25 cycles
72°C	1 min	
72°C	10 min	
4°C	∞	

The resulting PCR products were run on an agarose gel to confirm their presence and size (80 V, 60 min).

3.5 RNA hybridization and capture experiments

In order to confirm that the target 16S rRNA can be selectively enriched from the RNA pool following an ESP-based RNA extraction protocol, the following experiments were conducted.

3.5.1 General procedure

RNA extracted from *O. antarctica* cells was used for this test. Contaminating DNA had to be removed from the RNA samples, following the instructions of the *TURBO DNA-free kit* (Invitrogen):
10X TURBO Buffer (0.1 volume) and 2 μL TURBO DNase were added to the RNA preparation and mixed gently by tapping. The mixture was incubated at 37°C for 30 min and 0.2 volume DNase Inactivation Reagent were added. The preparation was incubated at RT for 5 min while mixing occasionally and centrifuged at 10 000 rcf for 1.5 min. The supernatant was transferred into a fresh RNase-free tube.
For all experiments, the hybridization buffer was added to the samples to a final volume of 100 μL. For the capture experiments, 5 μL bio-Universal probe (50 pmol, bio-Universal) was added to the samples after the denaturing step, except for procedure D (outlined in tab. 3.6), were the probe was given to samples prior to denaturation. The bio-Universal probe was replaced with 5 μL hybridization buffer for negative control samples.
Streptavidin-coated beads were used for the capture experiments. The RNA was hybridized with a bio-Universal probe that binds to the target RNA sequence. The hybridized complex attached then to the magnetic beads through streptavidin-biotin binding. Major steps of the hybridization and capture experiments are outlined in figure 3.2.

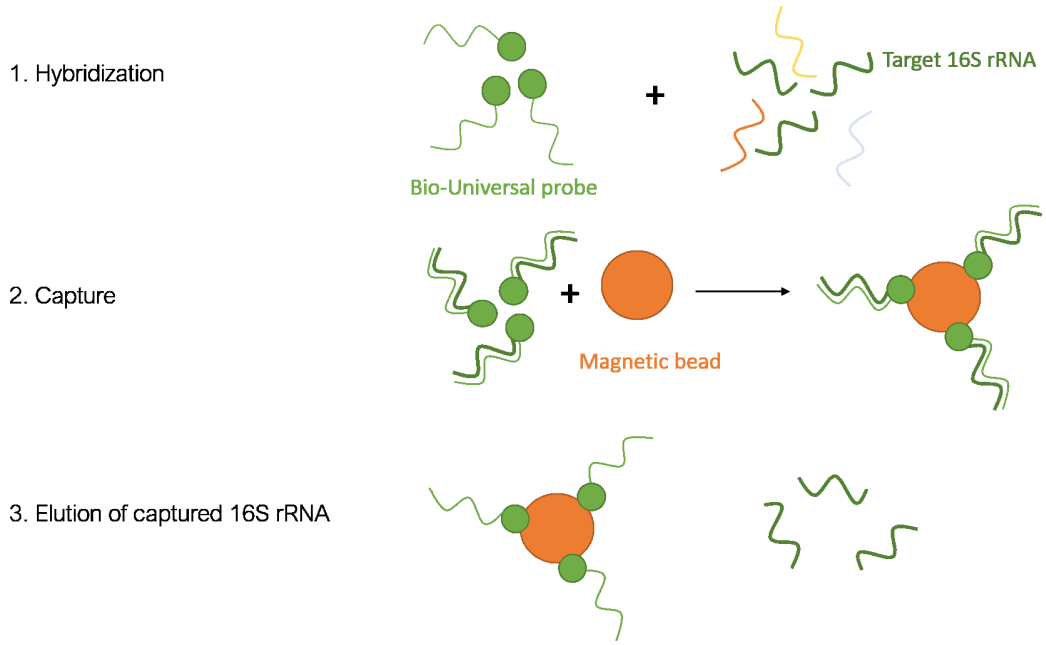

Figure 3.2: Schema of the major steps for the hybridization and capture experiments.

Table 3.6: Protocols that were followed for the RNA hybridization and capture approach with different buffers. RT: room temperature (21°C); HBI: 5x saline-sodium citrate (SSC) (25% formamide); HBII: 5x SSC; ESP: 1:1 mixture of ESP lysis buffer and ESP lysis diluent; HBU: hybridization buffer with urea (100 mM).

Procedure	Buffer	Denaturation	Hybridization
A	HBI	10 min 70°C	20 min RT
B	HBI	10 min 70°C 30 min RT	Overnight RT
C	HBII	10 min 70°C 30 min RT	Overnight RT
D	HBII	5 min 65°C	15 min RT
E	ESP	10 min 100°C	30 min 27°C
F	ESP	5 min 85°C	10 min RT
G	HBU	5 min 85°C	10 min RT

Preparation of beads

One volume of 0.5x SSC was given to the bead solution and mixed well. The beads were separated on a magnetic stand and the supernatant discarded. After that, the beads were resuspended in 500 μL 0.5x SSC, separated on a magnetic stand and the supernatant discarded. This step was repeated once. Finally, the beads were resuspended in one volume of 0.5x SSC.

Procedure

Bead solution (25 μL, MyOne C1, Oslo, Norway, if not otherwise stated) was added to the hybridized RNA samples and incubated at RT for 20 min. The beads were pulled out using a Dyna bead magnetic stand and the supernatant was transferred into a fresh 1.5 mL RNase-free tube (unbound RNA-samples). The samples were kept on ice until further usage. The magnetic beads were resuspended in DEPC-treated water, volume of the original RNA, the RNA eluted from the beads by incubating them at 90°C for 3 min at 300 rpm, separating on a magnetic stand and transferring the supernatant into a fresh RNase-free 1.5 mL tube (captured RNA-samples).

RNA clean-up

For the clean-up and concentration of the unbound RNA-samples the instructions of the *RNA Clean & Concentrator kit* (Zymo) were followed.
Two volumes (250 μL) of RNA binding buffer were added to the samples (volume of 125 μL), followed by 1 volume (375 μL) of 100% ethanol. The mixture was transferred into a Zymo-Spin IC column (with collection tube), centrifuged (10 000 rcf, 1 min, RT) and the flow-through discarded. RNA-prep buffer (400 μL) was added to the mix, centrifuged and the flow-through discarded. Then 700 μL wash buffer were added, the mixture centrifuged (10 000 rcf, 1 min), the flow-through discarded and the column centrifuged again (12 000 rcf, 2 min). The RNA samples were eluted in their original volume. Nanodrop and an agarose gel (1.5%, 5 μL of sample, 80 V, 60 min) were performed.

3.5.2 Effect of buffer composition and hybridization conditions

For determining optimal hybridization conditions different hybridization buffer were tested. All samples were prepared in duplicates. Negative controls were included for all experiments.
Four different hybridization buffers were used. The buffers differed mainly in content of denaturing agent, surfactant and salt content and are named Hybridization buffer I (HBI), Hybridization buffer II (HBII), ESP and Hybridization buffer with urea (HBU). Their compositions are outlined in table 3.7.

Table 3.7: Composition of the different hybridization buffers used for the RNA capture approach. HBI: Hybridization buffer I (5x saline-sodium citrate (SSC), 25% formamide); HBII: Hybridization buffer II (5x SSC); ESP mix: mixture of ESP lysis diluent and ESP lysis buffer; HBU: Hybridization buffer with urea (100 mM).

component	HBI (25% formamide)	HBII	ESP	HBU
NaCl	750 mM	750 mM		300 mM
EDTA			15 mM	1 mM
NaH_2PO_4				20 mM
Tris-Cl			50 mM	
Sodium-citrate	75 mM	75 mM		
SDS	0.02%	0.02%	0.2%	
Sarkozyl	0.1%	0.1%	2%	
GuSCN			1.5 M	
Formamide	25%			
urea				100 mM
pH			8.9	

All buffers were syringe-filtered after preparation (0.22 μm). The different procedures and buffers used are outlined in table 3.6.

In order to assess the effect of hybridization buffer on the capture efficiency, procedure B and C and procedure F and G (tab. 3.6) were compared to each other.

3.5.3 Effect of probe concentration

The effect of probe concentration was evaluated by two independent experiments. First, the HBII buffer and probe concentrations of 2.5 and 12.5 pmol, following procedure D (tab. 3.6) were used. In a second experiment, ESP buffer was used with probe concentrations of 2.5 and 12.5 pmol, following procedure F (tab. 3.6).

3.5.4 Effect of RNA concentration

In order to mimic expectable amounts of RNA in real seawater, the RNA content was reduced. The effect of RNA concentration was evaluated by using HBI buffer with 6 μg RNA, following procedure A (tab. 3.6) compared to HBI buffer with 0.5 μg RNA, following procedure B (tab. 3.6).

3.5.5 Effect of magnetic bead type

Three different types of beads, *MyOne C1, M-270 Streptavidin coated beads* (M-270) and *BD IMag^{TM} Streptavidin Particles Plus - DM* (BD IMag) were compared in this experiment. Their size and binding capacity for single stranded oligonucleotides (if known) are outlined in table 3.8. M-270 and BD IMag were compared using HBII

Table 3.8: Different bead types used for the capture experiments with size and binding capacity (if known) for single stranded (ss) oligonucleotides (oligo-nt).

Bead type	Size	Binding capacity (ss oligo-nt)
Myone C1	1 μm	$\sim$ 500 pmol
M-270	2.8 μm	$\sim$ 200 pmol
BD $IMag^{TM}$	0.2 μm	not tested

Table 3.9: Sequences of the used morpholino probes installed on the SPR sensors.

Morpholino Probe	Sequence (5'-3')
Negative control	CCTACCAAGTCAACATTGGTATAT- /SH/
Oleispira (detection probe)	CTAGCTAATCTCACTCAGGCTCAT- /SH/
Universal	TGTAGCGGTGAAATGCGTAGA- /SH/

buffer, following procedure B (tab. 3.6). Procedure E (tab. 3.6) was performed to compare M-270 and MyOne C1 beads.

3.6 SPR experiments

A portable SPR instrument as briefly described in the background section and outlined in [6] was used. The sensors used on this instrument were coated by an external collaborator at the University of Washington using morpholino probes as outlined in table 3.9.

A 24-nt long morpholino probe was immobilized on the sensors surface as detection probe. The morpholino probes (purchased from Gen Tools LLC, Philomath, OR, USA) have a 3'-disulfid-amid modification to attach them to the sensors' surface.

3.6.1 General procedure

Before starting the instrument, the waste tank was emptied and ensured that running buffer and regeneration solution tanks were filled. The connection between instrument and laptop was established. A flush step, followed by a 3 s pressurizing and a flow step, was included to confirm that the tubes were unclogged and did not contain air. The running buffer was injected at the beginning of the experiments, followed by a flow step until the signal on the sensors had stabilized. Pre-set fluidics programs were used for the different experiments. The samples were injected in a volume of 0.5 mL and the RIU recorded in real-time. Positive controls were included to confirm the quality of the sensors. The running buffer was injected after finishing the experiments, to rinse the system before shutting down.

Table 3.10: Sequences of used oligonucleotides. REF: positive control (Oleispira oligo); Universal: Universal oligo; MM2: 2-mismatch Oleispira oligo; MM1: 1-mismatch Oleispira oligo; PC: positivecontrol, combined oligo; iSP18: internal spacer (18-mer hexa-ethyleneglycol). Mismatches in oligos are underlined and in bold.

sample	Sequence (5'-3')
REF	ATGAGCCTGAGTGAGATTAGCTAG
Universal	TCTACGCATTTCACCGCTACA
MM2	ATGA**A**CCTGAGTTAGAT**T**AGCTAG
MM1	ATGA**A**CCTGAGTGAGATTAGCTAG
PC	ATGAGCCTGAGTGAGATTAGCTAG /iSP18/TGTAGCGGTGAAATGCGTA

3.6.2 Effect of buffer composition on specificity

Synthetic oligonucleotides with different number of mismatches to the Oleispira probe (tab. 3.9) were used in order to observe the SPR sensors' specificity under different buffer conditions. The buffers used differed in salt concentration, content of surfactant and denaturing agent. Results were recorded on sensor 2 (Universal), sensor 3 (negative control) and sensor 4 (Oleispira). A 24-nucleotide long oligo, 100% complementary to the detection probe on sensor 4, was used as a positive control (REF) for the analysis. For further testing of the sensors' specificity a Universal oligo (100% complementary to sensor 2), a 1-mismatch (MM1) and 2-mismatches (MM2) containing oligo were used. Their sequences are outlined in table 3.10.

The oligo stocks (1 mM) were either directly used or further diluted in the corresponding running buffer.

Buffers

The Dulbecco's phosphate buffered saline (DPBS) contains KCl (0.2 g/L), NaCl (8.0 g/L), KH_2PO_4 (0.2 g/L), and anhydrous Na_2HPO_4 (1.15 g/L), DPBS-T supplemented with 0.1% Tween 20, DPBS-U supplemented with 200 mM urea and high salt DPBS having a NaCl content of 29.2 g/L (500 mM). All chemicals were purchased from Sigma-Aldrich if not otherwise stated. All buffers were syringe-filtered after preparation (0.22 μm). A 50 mM NaOH denaturing solution was used for regenerating the SPR surfaces.

Procedure

Synthetic oligos (2.5 μL, 100 μM) were mixed with 495 μL buffer prior to injection. The appropriate fluidics program was selected in the control software and the sample run was initiated. When summoned by the fluidics program, the sample was injected. Changes in RIU-values (i.e. the binding curves of each target analyte) were recorded in real-time and analyzed with a custom R script. Analysis of the samples

Table 3.11: Fluidics program used for SPR specificity experiments.

Step	Time (s)	Pump Speed ($\mu L/min$)
Flow	120	120
Baseline	0	0
Injection	10	10
Flow	240	20
Flush	7	0
Flow	120	20
Regenerate	120	100
Flow	120	100

was performed following the fluidics program outlined in table 3.11, with a total duration time of 12 min for each measurement.

Different oligos were injected and their RIU values recorded after 367 s. First, the positive control (REF) was injected, followed by the Universal probe (Uni), the MM2, the MM1 and the Oleispira oligo (tab. 3.10) all of which, excluding REF, were diluted 10x in the running buffer. A buffer injection was included between different samples and recorded as well. All measurements, except for REF, were carried out in triplicates. REF was measured to begin and end of the experiment in order to control the quality of the sensors. Signals on different sensors were compared to each other and their ratios were calculated.

3.6.3 Detection of combined oligos

In order to confirm the potential of ESP as a buffer for the detection of oligonucleotides in the SPR experiments, two amplification strategies, namely the sequential and the capture approach, as outlined in [6], were performed. Results were recorded on sensor 1 (negative control) and sensor 3 (Oleispira).

Preparation

The combined oligo stock (1 mM) and the bio-Universal probe (1 mM) were used and diluted in DPBS (100 μM). Dilutions of the combined oligo (1 μM) were prepared in DPBS and ESP mix. For the bead amplification BD IMag beads were used. The beads were washed twice and resuspended in DPBS-T prior to usage. DPBS-T was used as a running buffer. The samples were injected in either DPBS-T or ESP mix. The ESP mix is a 1:1 mixture of the ESP lysis diluent and the ESP lysis buffer (see tab. 3.7). A 50 mM NaOH solution was used for regenerating the sensors' surfaces.

Procedure

Sequential approach

Table 3.12: Fluidics program 2 used for amplification and PCR product detection.

Step	Time (s)	Pump Speed (μL/min)
Flush	7	0
Flow	120	30
Baseline	0	0
Injection	10	0
Flow	240	30
Flush	7	0
Flow	120	30
Injection	10	0
Flow	600	30
Flush	7	0
Flow	120	30
Regenerate	240	100
Flow	240	100

Table 3.13: Fluidics program 3 used for rinsing the sensors with 8 M urea and running buffer.

Step	Time (s)	Pump Speed (μL/min)
Flow	10	30
Baseline	0	0
Flow	10	30
Injection	10	0
Flow	120	30
Flush	7	0
Flow	60	30
Regenerate	120	100
Flow	240	100

The combined oligo was diluted 1000x and the bio-Uni probe 10x in DPBS. Then, 2.5 μL of each where given to a fresh 1.5 mL eppendorf tube and allowed to hybridize for 20 min at RT. After the incubation, 495 μL buffer were added and the mixture injected, following the fluidics program 2 as outlined in table 3.12. The samples were either injected in DPBS-T or ESP mix. Meanwhile, 25 μL of washed beads were mixed with 475 μL DPBS-T and injected after 4 min (tab. 3.12). All measurements were carried out in triplicates. A 8 M urea injection (fluidics program 3, tab. 3.13) was carried out between samples and the injection port rinsed with DPBS-T afterwards.

Capture approach

The combined oligo was diluted 100x and the bio-Uni probe 10x in DPBS. Then, 2.5 μL of each were given to a fresh 1.5 mL eppendorf tube and allowed to hybridize for 20 min at RT. After the incubation, 25 μL washed beads were given to the mixture and allowed to hybridize for 10 min at RT. Then, 470 μL ESP buffer were given to

Table 3.14: Fluidics program 1.

Step	Time (s)	Pump Speed (μL/min)
Flow	120	30
Baseline	0	0
Injection	10	0
Flow	600	30
Flush	7	0
Flow	120	30
Regenerate	120	100
Flow	120	100
Regenerate	120	100
Flow	120	100

the sample and the mixture was put on a magnetic stand to pull out the conjugated beads. The beads were washed twice with 500 μL DPBS-T and then resuspended in the same volume. The mixture was injected after 2 min and RIU values were recorded after 12 min, following the fluidics program 1 as outlined in table 3.14. A 8 M urea injection (fluidics program 3, tab. 3.13) was carried out between samples and the injection port rinsed with DPBS-T.

3.6.4 Detection of PCR products

Aiming to detect 16S rRNA, which is approximately 1500 bp long, experiments with longer targets were conducted. PCR products were generated from gene fragments, mimicking the target 16S rRNA with a length of 90 and 477 bp respectively. The *gBlock® Gene Fragments* were obtained from *Integrated DNA Technologies* (Coralville, Iowa, USA) and treated according to the manufacturer's instructions. Per PCR reaction 10 ng were used.

Probes

A combined oligo with an internal spacer (18-mer hexa-ethylene-glycol) was used as positive control for the PCR detection experiments. Its sequence is outlined in table 3.10. The gene fragments sequences can be found in the appendix.

Procedure

The PCR products (2.5 μL) were incubated for 1 min at 95°C and cooled for another minute on ice. Then, 2.5 μL bio-Uni probe were given to the sample and incubated for 10 min at RT. After the incubation, 495 μL DPBS-T buffer was added and the sample mixed well. The sample was injected following fluidics program 2 (tab. 3.12), followed by injecting 25 μL of washed beads (in 475 μL DPBS-T). The combined oligo (1 μM) was incubated and injected in the same way, in order to serve as a positive control. A 8 M urea injection (fluidics program 3, tab. 3.13) was carried out after the samples run and the injection port rinsed with DPBS-T. RIU values were recorded

after 18 min (fluidics program 2). The bead background (beads conjugated with bio-Uni probe) was subtracted from obtained values.

4 Results

To ensure appropriate growth, the OD_{600} was tracked of the Oleispira cultures. Their cell numbers and RNA content were determined using different methodical approaches. RNA was extracted from observed cells with two commercially available and an ESP compatible method. Success was proven with two primers, specific towards sequences within the Oleispira rRNA sequence, and gel electrophoresis. Furthermore, target 16S rRNA was tried to be selectively enriched out of a pool of RNA testing different hybridization procedures. To test the abilitiy of the SPR sensors to distinguish highly similar sequences, experiments with mismatched oligos and different running buffers were conducted. Two amplification strategies were tested and compared to confirm that ESP compatible buffer solution can be used for binding of the target analyte. One of the amplification strategies was further used to test the ability to detect longer molecules.

4.1 Oleispira cultivation

As a psychrophilic bacterium, *O. antarctica* is adapted to cold-water environments. In order to observe the effect of temperature on its growth, two cultures were prepared and their growth observed at 4 and 12°C respectively. To confirm growth and presence of uniform cells, fluorescence microscopy was employed.

4.2 Maintenance routine and quality control

The presence of Oleispira cells in the cultivated cultures was confirmed with DAPI fluorescence microscopy. Rod-shaped cells could be observed (fig. 4.1).

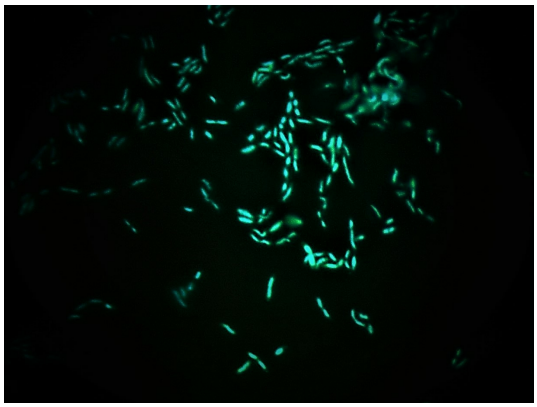

Figure 4.1: DAPI-stained Oleispira cells under a fluorescence microscope.

A spectrophotometer was employed to measure the OD_{600} of samples to give information about their growth and concentration. The measured light intensity is inversely proportional to the concentration of bacteria in the sample. Further on, this method was employed to confirm growth of cultures prior to RNA extraction. The maximum OD_{600} observed with the culture grown at 12°C was 2.5x higher than of the culture at 4°C. The 4°C culture had a slow increase of OD_{600} until day 10 of incubation, from day 10 to day 12 the OD_{600} increased stronger and yielded a maximum OD_{600} of 0.380 (fig. 4.2). From day 12 until the end of measurements the cultures' OD_{600} increased slower. The 12°C culture had a moderate increase in OD_{600} until day 5 of incubation after which the OD_{600} increased faster until day 12 with a maximum OD_{600} of 1.036 (fig. 4.3). From day 12 until the end of measurements, the OD_{600} stabilized. The standard deviations increased with increasing incubation time and OD_{600}.

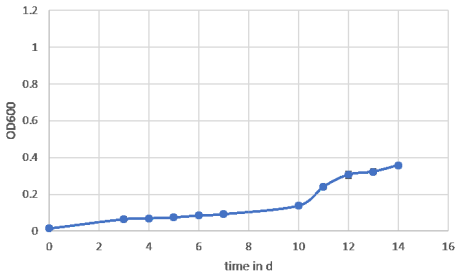

Figure 4.2: Growth curve of *O. antarctica* at 4°C, incubated in the dark on a rotator for 14 days.

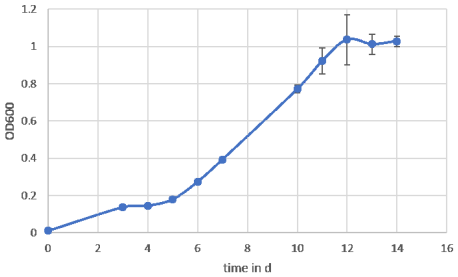

Figure 4.3: Growth curve of *O. antarctica* at 12°C, incubated in the dark on a rotator for 14 days.

4.3 Quantification

The quantification of bacterial cells is crucial for understanding their growth, determining cell numbers and for comparison to other bacteria.

Most probable number

A modified version of this method, as previously described, was employed to estimate the order of magnitude of cell numbers of *O. antarctica* based on dilution to extinction. Cultures of *O. antarctica* were serially diluted to a factor of 10^{-10}. Growth could be observed in test tubes until a dilution factor of 10^{-7}. The 10^{-7}-dilution started to get turbid after day 5 of incubation. After 12 days of incubation, the OD_{600} of the samples in which growth had occurred were somewhat variable with values ranging from 0.55 – 0.900 (fig. 4.4, fig. 4.5). The blanks' turbidity started to increase after day 10 of incubation. Therefore, values of the 10^{-10} diluted culture were further used as blank. The more diluted the cultures were, the more time they needed to show growth.

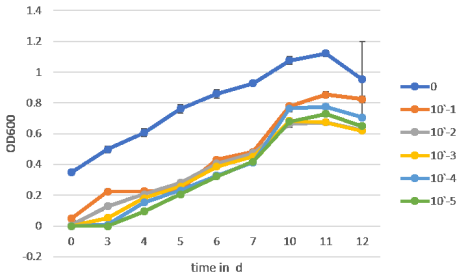

Figure 4.4: Absorbance (OD_{600} of serial dilution until 10^{-5} of *O. antarctica* against time. Error bars show ± s.d., 0: original culture; 10-1 10x diluted culture, 10-2: 100x diluted culture, 10-3: 1000x diluted culture, 10-4: 10^4 diluted culture, 10-5: 10^5 diluted culture.

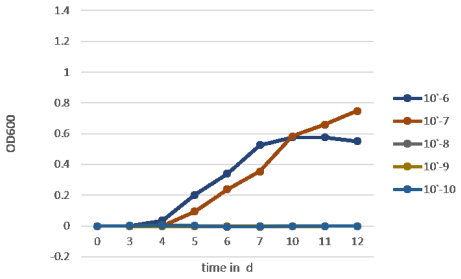

Figure 4.5: Absorbance (OD_{600} of serial dilution until 10^{-10} of *O. antarctica* against time. Error bars show ± s.d., 10-6: 10^6 diluted culture, 10-7: 10^7 diluted culture, 10-8: 10^8 diluted culture, 10-9: 10^9 diluted culture, 10-10: 10^{10} diluted culture.

Plate counting

Cell numbers from samples in solutions are usually too high to be counted, therefore these are diluted serially and further plated to obtain countable colonies. For determining cell numbers, 100 μL of the 10^{-2} to 10^{-5} culture were plated. After 5 days of incubation all cultures showed colonies. The colonies of the 10^{-5} culture were counted for one quadrant and multiplied by 4 to determine the cell number

per plate. The average number of colonies per plate was 454. Involving the dilution factor of 10^5, the original culture had 4.5 x 10^8 cells per mL.

Flow Cytometry

The cell numbers of the Oleispira culture were estimated with flow cytometry and compared to the numbers obtained with the plate counting method. The dilutions of 10^{-2} to 10^{-4} were observed. A blank, containing filtered seawater, was included and subtracted from obtained values. With decreasing dilution, the estimated cell numbers increased (tab. 4.1). The obtained estimated cell numbers were in the same range of magnitude as the values obtained with the plate counting method.

Table 4.1: Data obtained from flow cytometry of a serial dilution of an *O. antarctica* culture to estimate cell numbers per mL. s.d. = standard deviation.

Dilution	**Average amount of cell numbers (± s.d.)**	**Estimated cell numbers per mL (± s.d.)**
10^{-4}	2215 ± 24.5	$4.43 \times 10^8 \pm 4.9 \times 10^6$
10^{-3}	28947 ± 755	$5.79 \times 10^8 \pm 15.1 \times 10^6$
10^{-2}	308647 ± 293	$6.17 \times 10^8 \pm 0.6 \times 10^6$

Estimation of total RNA content

Oleispira cells were pelleted and their RNA extracted. A serial dilution was made from the obtained pellet and plated to obtain total cell numbers. Both methods were done in order to cross-validate numbers.
The plots obtained with flow cytometry showed two populations for the stained dilutions (fig. 4.6) in all samples, when plotting the forward scatter against the fluorescence emission. In brown the background noise, obtained with FSW, is illustrated, while stained cells can be seen in black. Obtained events from background and samples appeared to have the same size (FSC), wherefore samples were distinguished from the background according to fluorescence intensity.

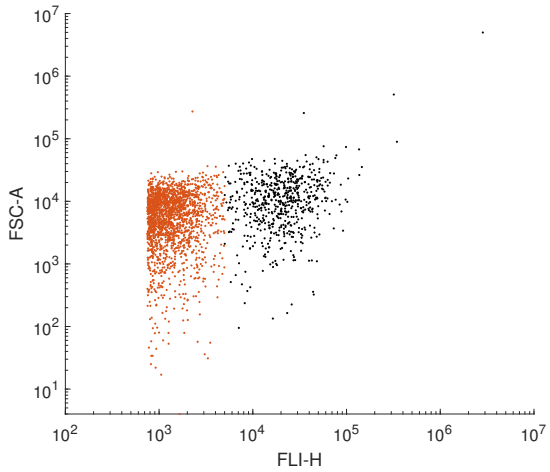

Figure 4.6: Plot of forward scatter against fluorescence emission (logarithmic scale) obtained with a flow cytometer of stained 10^4 diluted Oleispira in filtered seawater (FSW). Brown: background noise from stained FSW, subtracted from values; Black: events of stained sample other than background.

Values resulting from background noise were subtracted from the stained samples. The samples were measured in triplicates and the results of the cell count can be seen in table 4.2.

Table 4.2: Data obtained from flow cytometry of a serial dilution of an *O. antarctica* culture to estimate cell numbers per mL. s.d. = standard deviation.

Dilution	**Average amount of cell numbers (± s.d.)**	**Estimated cell numbers per mL (± s.d.)**
10^{-4}	1766 ± 106	$3.5 \times 10^8 \pm 2.1 \times 10^7$
10^{-3}	14034 ± 568	$2.8 \times 10^8 \pm 1.1 \times 10^7$
10^{-2}	115367 ± 5119	$2.3 \times 10^8 \pm 1.0 \times 10^7$

In order to determine the RNA content per cell, dilution series of the same Oleispira culture as observed with flow cytometry were made and plated directly after harvesting the cells. The Oleispira culture was plated in dilutions from 10^{-4} to 10^{-7}. Estimated cell numbers were one order of magnitude lower than cell numbers obtained with flow cytometry (tab. 4.3). No growth occurred in the plated 10^{-7} cultures, 8 colonies could be observed on average on the 10^{-6} plates, 50 on the 10^{-5} and 259 on the 10^{-4} plates. The estimated cell numbers obtained with this method reached from 2.6 to 8 x 10^7 cells in 1 mL culture, compared to values of 2.3 to 3.5 x 10^8 cells obtained with flow cytometry. Values from the plate counting were further taken for estimating the total RNA content per cell.

Table 4.3: Data obtained with plate counting of a serial dilution of an *O. antarctica* culture to estimate cell numbers per mL. s.d. = standard deviation.

Dilution	Average amount of cell numbers (± s.d.)	Estimated cell numbers per mL (± s.d.)
10^{-4}	259 ± 9.5	$2.6 \times 10^7 \pm 3.8 \times 10^6$
10^{-5}	50 ± 0.8	$5 \times 10^7 \pm 0.8 \times 10^6$
10^{-6}	8 ± 3.6	$8 \times 10^7 \pm 35.6 \times 10^6$
10^{-7}	no growth	-

4.4 RNA extraction

An ESP compatible method to extract RNA was tested and compared to commercially available methods.

ZymoBIOMICS method

Many methods exist to extract RNA and DNA. The extracted RNA can be further used to determine the RNA content per cell if combined with plate or cell counting methods. In order to get RNA and DNA of the same organism the Zymo BIOMICS protocol was followed. The extraction of DNA and RNA was successful. The extractions were carried out in quadruplets and run on an agarose gel to confirm their quality (fig. 4.7). Only two of the four DNA samples were run on the gel, since obtained concentrations with nanodrop revealed similar results (tab. 8). The extraction was successful, both DNA and RNA could be extracted. The RNA content was 4x as high as the extracted DNA content (tab. 8).

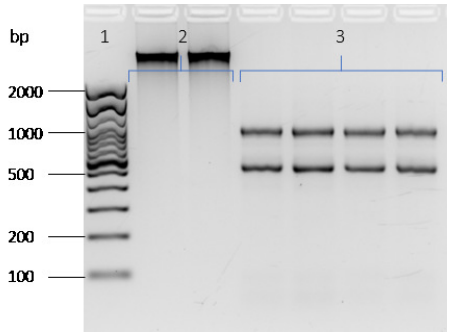

Figure 4.7: 1.5% Agarose gel of DNA/RNA extraction following the Zymo BIOMICS protocol. 1: TrackIt 100 bp ladder, 2: extracted Oleispira DNA; 3: extracted Oleispira RNA.

The average estimated RNA concentration was 78 ng/μL which corresponds to an RNA content of 302 fg per cell. The RNA content was estimated using cell numbers obtained with plate counting of the 10^{-4} culture. Cell numbers were calculated

based on the DNA content and genome size (4.4 Mbp [43]) of *O. antarctica*. Based on this calculation, the culture contained 4.3 $\times$ 10^8 cells per mL, comparable to the cell numbers obtained with flow cytometry.

ESP compatible method

The 3G ESP employs the buffer ESP for the extraction of the bacterial RNA. To check whether this extraction method could yield the same results as commercially available extraction methods, the ESP protocol was compared with the PureLink protocol. The success of each extraction was further confirmed with RevT-PCR.

The quality control with gel electrophoresis revealed that RNA was extracted from samples with both methods (fig. 4.8). The PureLink extracted RNA showed two bands in each sample, while in all replicates of the ESP extracted RNA only a smear appeared on the gel.

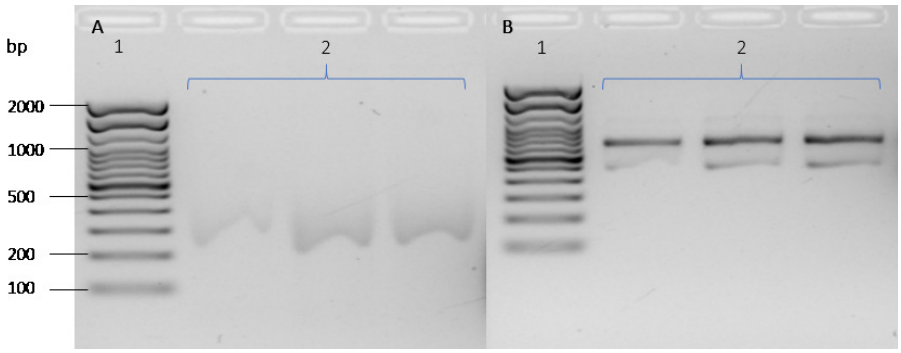

Figure 4.8: 1.5% Agarose gel of RNA extraction following the ESP (A) and the PureLink (B) protocol, with on-column DNase treatment. 1: TrackIt 100 bp ladder, 2: extracted Oleispira RNA.

4.5 Verifying the presence of target 16S rRNA fragment

The primers used were specific towards sequences within *O. antarcticas* rRNA sequence (appendix). To prove the success of the RNA extraction with the proposed primers, a RevT-PCR was run. The PCR was run with Oleispira oligo and Universal probe as primers (tab. 3.5). The resulting PCR products are shown in figure 4.9. Negative and positive controls were included.

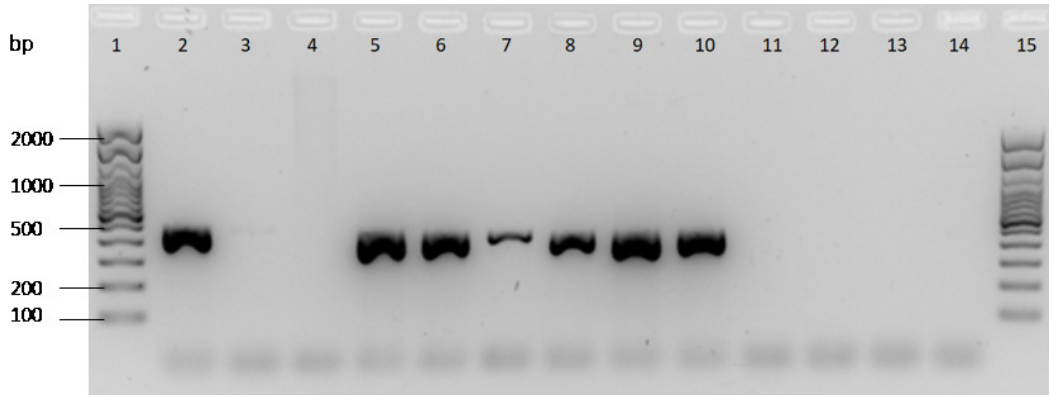

Figure 4.9: PCR products of RNA extraction of *O. antarctica* with ESP and PureLink Zymo kit. 1, 15: TrackIt 100 bp ladder; 2: positive control (Oleispira DNA); 3: negative control (OLN3 RNA); 4: negative control (OLN3 DNA); 5: extracted RNA with PureLink Zymo kit (Zymo) after reverse transcription (RevT); 6: extracted RNA with ESP (ESP) after RevT; 7: Zymo no template control (NTC) after RevT; 8: ESP NTC after RevT; 9: DNase treated Zymo RNA; 10: DNase treated ESP RNA; 11: DNase treated Zymo NTC; 12: DNase treated ESP NTC; 13: RevT negative control PCR-NTC; 14: PCR NTC.

The observed bands (lane 5-10) were at the same height as the band obtained with the positive control (lane 2). The bands of the non-DNase treated RevT-NTC (lane 7, 8) were weaker than those observed with the samples that contained extracted RNA.

4.6 RNA capture

Different hybridization procedures were tested to selectively enrich target 16S rRNA out of an RNA-pool.

4.6.1 Effect of buffer composition and hybridization conditions

The detection of the target 16S rRNA out of the extracted RNA-pool is challenging. Hence, hybridization and capture conditions have to be optimized. In the experiment performed for RNA hybridization, different hybridization protocols and buffers were used. The RNA was captured using magnetic beads. The supernatant from that capture is referred to as unbound samples, while the RNA that bound to the beads and that was further eluted is referred to as captured samples.

The results of the capture approach with HBI, following procedure A (tab. 3.6), are shown in figure 4.10. The bands of the unbound samples showed the same intensity as the starting material (fig. 4.10, lane 2-4) and did not differ between the test and control samples. The captured test samples showed a light band under the expected 16S rRNA band (lane 5, arrows), while one of the captured control samples (lane 6, arrow) showed a band at the height of the 23S rRNA.

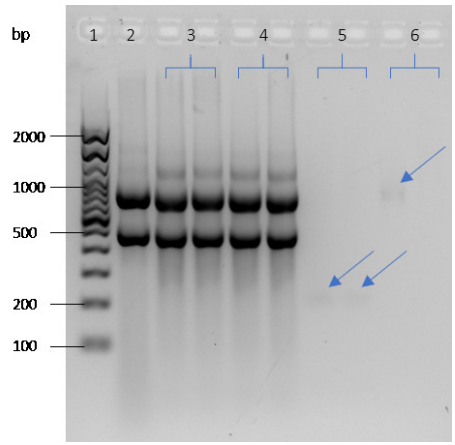

Figure 4.10: 1.5% Agarose gel of RNA capture approach with 5x SSC (HBI, procedure A). 1: TrackIt 100 bp ladder; 2: starting material (Alcanivorax, OLN3); 3: unbound test RNA (UB RNA-1, UB RNA-2); 4 unbound control RNA (UB RNA-3, UB RNA-4); 5: captured test RNA (CP RNA-1, CP RNA-2); 6: captured control RNA (CP RNA-3, CP RNA-4). Arrows show captured rRNA.

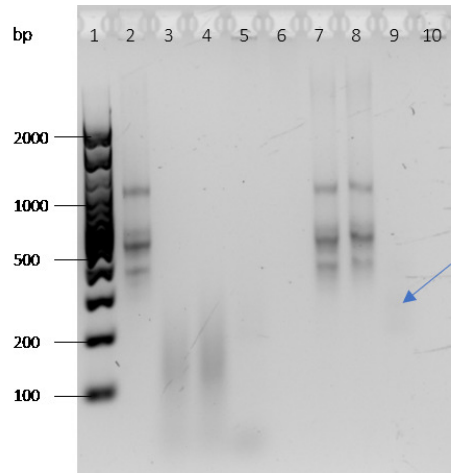

Figure 4.11: 1.5 % Agarose gel of RNA capture approach with ESP (procedure E) and 5x SSC (HBI; procedure B). 1: TrackIt 100 bp ladder; 2: starting material; 3: unbound test RNA in ESP (U ESP 1); 4: unbound control RNA in ESP (U ESP 3); 5: captured test RNA in ESP (C ESP 1); 6: captured control RNA in ESP (C ESP 3); 7: unbound test RNA in HBI (U HB 1); 8: unbound control RNA in HBI (U HB 3); 9: captured test RNA in HBI (C HB 1); 10: captured control RNA in HBI (C HB 3). The arrow shows captured 16S rRNA.

The same overnight protocol as used for HBI was used with HBII (fig. 4.12, procedure C). The unbound test and control samples showed distinct bands similar to those that could be observed with the starting material (lane 3, 4, 5). The RNA was eluted in 13 μL, which corresponds to a 4.6x dilution of the RNAs' original volume (2.8 μL). Nanodrop analysis revealed that the unbound samples had a higher concentration than their captured equivalents. The difference in concentration between the captured test and control samples was very high (lane 6, 7), with the test samples

having 4x higher values than the control samples (tab. 3). Two weak bands could be observed in the captured test sample (lane 6), which could not be found in the control (lane 7). The higher band appeared at the height of the 16S rRNA, while the lower band was below the 100 bp band.

The overnight protocols (procedure B and C) yielded better results in terms of captured RNA content. Comparing the two buffers used, the HBII yielded higher concentrations of 16S rRNA than HBI.

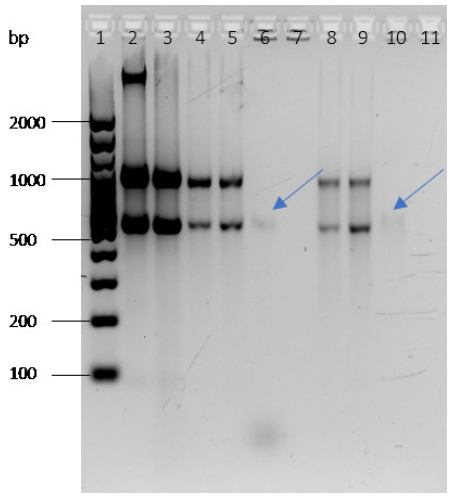

Figure 4.12: Agarose gel (1.5 %) of RNA capture approach with 5x SSC (HBII; procedure C) and hybridization buffer with urea (HBU; procedure G). 1: TrackIt 100 bp ladder; 2: starting material, not Dnase treated; 3: Dnase treated starting material; 4: unbound test RNA in HBII (U HBII 1); 5: unbound control RNA in HBII (U HBII 3); 6: captured test RNA in HBII (C HBII 1); 7: captured control RNA in HBII (C HBII 3); 8: unbound test RNA in HBU (U HBU 1); 9: unbound control RNA in HBU (U HBU 3); 10: captured test RNA in HBU (C HBU 1); 11: captured control RNA in HBU (C HBU 3). Arrows show captured 16S rRNA.

Another approach used buffer with urea as denaturing agent (fig. 4.12). The captured test sample (lane 10) showed a weak band on height of the 16S rRNA band that could be found in the starting material (2, 3) and the unbound samples (test: lane 8, control: lane 9). Both unbound samples showed two distinct bands, the lower one at the height of 500 bp and the higher one at the height of 800 bp. The captured test and control sample (lane 10, 11) showed a band at the top of the gel. The differences among the captured samples with use of HBU were not as high as with use of HBII (fig. 4.12, overnight incubation protocol). Only one of the test samples “C HBU 1" (tab. 3) showed a 2x higher concentration, while “C HBU 2" yielded the same amount as the control samples. The unbound test and control samples did not differ among each other, neither with HBII nor with HBU as hybridization buffer

4.6.2 Effect of probe concentration

The ratio of probe content to amount of sample is important to avoid saturation of the beads through too high concentrations of unhybridized probe. Therefore, different concentrations of probe were used in the capture experiments.
The probe concentration was set to 50 pmol if not otherwise stated, which corresponded to a 100x excess of the target 16S rRNA. With HBII buffer following procedure C, bands below 100 bp (fig. 4.12) could be observed, an evidence for a high amount of unbound probe. Hence, probe concentrations of 12.5 and 2.5 pmol were tested.
The probe content was reduced in the experiments with HBII, following procedure D. It was also reduced in experiments with ESP, following procedure F (fig. 4.13, fig. 4.15).
With a 100x excess of probe compared to the target 16S rRNA (50 pmol, fig. 4.13) test samples of both buffer approaches (HBII and ESP) showed a smear below the 16S rRNA band. Only captured probes were run on this gel. The control samples (not containing RNA) revealed no band (lane 5, 7). The bands obtained with HBII appeared to be stronger than those obtained with ESP. Both captured test samples of the ESP approach showed a smear below the 100 bp band.

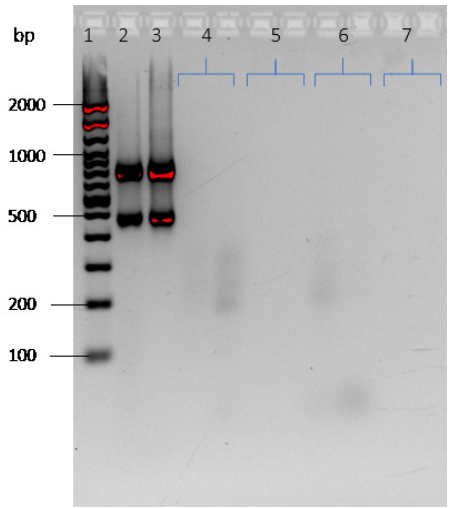

Figure 4.13: 1.5% Agarose gel of RNA capture approach with 5x SSC (HBII; procedure D) and ESP (procedure F). 1: TrackIt Ladder 100 bp; 2: starting material for HBII samples, RNA 4 from RNA extraction from 21/02/19; 3: starting material for ESP samples, RNA 1 from 21/02/19; 4: Captured test sample in HBII (C HBII 1, C HBII 2); 5: captured control sample in HBII (C HBII 3, C HBII 4); 6: captured test sample in ESP (C ESP 1, C ESP 2); 7: captured control sample in ESP (C ESP 3, C ESP 4).

With a probe content of 12.5 pmol (fig. 4.14) a weak band, around the 200 bp band (lane 3, arrow), could be observed in the test samples following procedure F (ESP).

The corresponding control samples did not show any band (lane 4). Both test samples in the HBII approach (procedure D) showed a band between 300 and 200 bp (lane 5, arrow), while the negative control samples did not show any band (lane 6). Lane 8 and 9 showed the biotinylated probe in ESP and HBII, which both yielded a band below the 100 bp band.

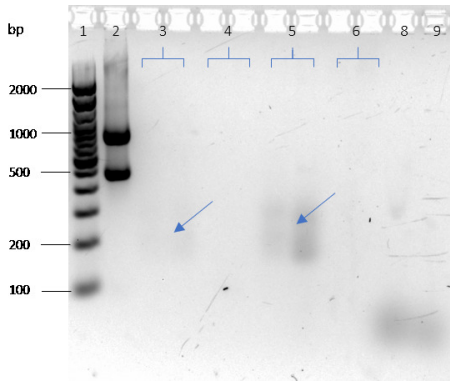

Figure 4.14: 1.5% Agarose gel of RNA-capture approach with ESP and HBII. The biotinylated probe was given to the samples in 50x extend (12.5 pmol). 1: Trackit 100 bp ladder; 2: starting material, Olei RNA 2 (21-02-2019); 3: captured test sample in ESP (C ESP 1, C ESP 2); 4: captured control sample in ESP (C ESP 3, C ESP 4); 5: captured test sample in HBII (C HBII 1, C HBII 2); 6: captured control sample in HBII (C HBII 3, C HBII 4); 7: biotinylated probe in ESP; 8: biotinylated probe in HBII. Arrows show captured 16S rRNA.

With a probe content of 2.5 pmol (fig. 4.15), no evaluable results could be obtained. The determined concentrations were similar between control and test samples and did not exceed 16 ng/μL for the test samples (tab. 7).

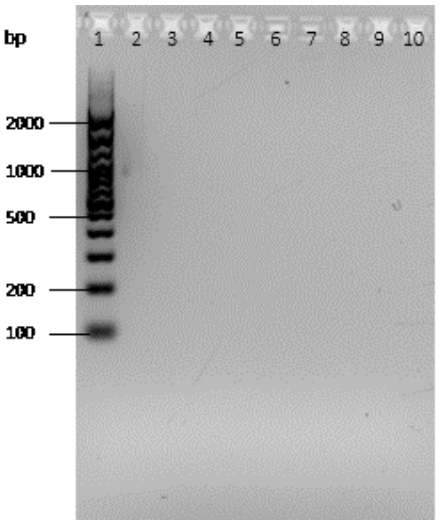

Figure 4.15: 1.5% Agarose gel of RNA-capture approach with 2.5 pmol probe concentration of the biotinylated probe and with HBII and ESP. 1: Trackit 100bp ladder; 2: starting material (RNA 1 from 21-02-2019); 3: 1st capture of ESP test sample (C ESP 1); 4: 1st capture of ESP control sample (C ESP 3); 5: 2nd capture of ESP test sample (C ESP I); 6: 2nd capture of ESP control sample (C ESP III); 7: 1st capture of HBII test sample (C HBII 1); 8: 1st capture of HBII control sample (C HBII 3); 9: 2nd capture of HBII test sample (C HBII I); 10: 2nd capture of HBII control sample (C HBII III).

4.6.3 Effect of RNA concentration

Using HBI as hybridization buffer, two different concentrations of RNA, 6 and 0.5 μg were tested. Results with HBI buffer, following procedure A and an amount of 6 μg RNA are shown in figure 4.10, while the results with 0.5 μg RNA, following procedure B are shown in figure 4.11. As described above, the captured test samples showed a light band under the expected 16S rRNA band, while one of the captured control samples showed a band at the height of the 23S rRNA. For procedure B, the unbound test and control samples showed the same bands as the starting material (fig. 4.11, lane 2, 7, 8). A light smear was visible in the captured test sample (lane 9), which was below the 16S rRNA band. The captured control sample showed a band at the top of the gel (lane 10), showing that high molecular weighted nucleic acids could not pass through the gel.

4.6.4 Effect of magnetic bead type

Different types of beads were used to investigate their effect on the RNA capture. For most of the experiments MyOne C1 beads were used. Two other types of beads, M-270 (fig. 4.13, 4.16) and BD IMag (fig. 4.16), were tested with the HBII protocol (procedure D). M-270 beads yielded evaluable results. As can be seen in figure 4.13 (lane 4) and figure 4.14 (lane 5), the test samples (containing RNA) could be captured. This could not be observed with the BD IMag (fig. 4.16, lane 4). Even though

unbound RNA (supernatant) was mixed with BD IMag beads for a second round of capture (lane 8, 9), no RNA could be captured with these beads.

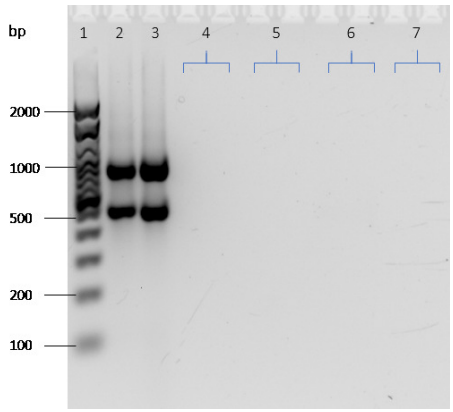

Figure 4.16: 1.5 % Agarose gel of RNA capture approach with HBII. 2.5 pmol biotinylated probe, BD IMag beads, double bead capture were used. 1: Trackit 100 bp ladder; 2: starting material (RNA 2 from 21-02-2019); 3: starting material (RNA 3 from 21-02-2019); 4: 1st capture of test sample (C HBII 1, C HBII 2); 5: 1st capture of HBII control sample (C HBII 3, C HBII 4); 6: 2nd capture of HBII test sample (C HBII I, C HBII II); 7: 2nd capture of HBII control sample (C HBII III, C HBII IV).

4.7 SPR experiments

4.7.1 Effect of buffer composition on specificity

The ability of a sensor to distinguish between target nucleic acid and highly similar sequences is critical. In the experiment performed for specificity testing, the effect of buffer composition was tested by measuring the signals of three different mismatch containing oligonucleotides on the Oleispira-specific sensor (sensor 4) and two negative control sensors (sensor 2 and 3) in different running buffers. MM1 containing one mismatched oligonucleotide compared to the 100% matching oligo, MM2 containing 2 mismatched oligonucleotides compared to the 100% matching oligo and Uni, containing 10 mismatches. Modifications of a phosphate buffered saline solution were compared to assess the effect of increased salt concentration, presence of denaturing agents and surfactants on the stringency of the hybridization. The RIU values after 367 s were recorded and the ratios of sensor 4 to sensor 3, sensor 4 to sensor 2 and sensor 3 to sensor 2 calculated. The different buffers yielded different RIU values and ratios, however they followed the same trend: the RIU values decreased with increasing number of mismatches (fig. 4.17). Experiments with lower salt concentrations in DPBS (2x and 10x diluted DPBS) yielded no evaluable result (fig. 4, fig. 5). In figure 4.17, the RIU values on sensor 4 of the SPR instrument after 6 min are shown. The RIU values were recorded for several oligos in four different buffers. The average buffer signal was considered as background and subtracted from values.

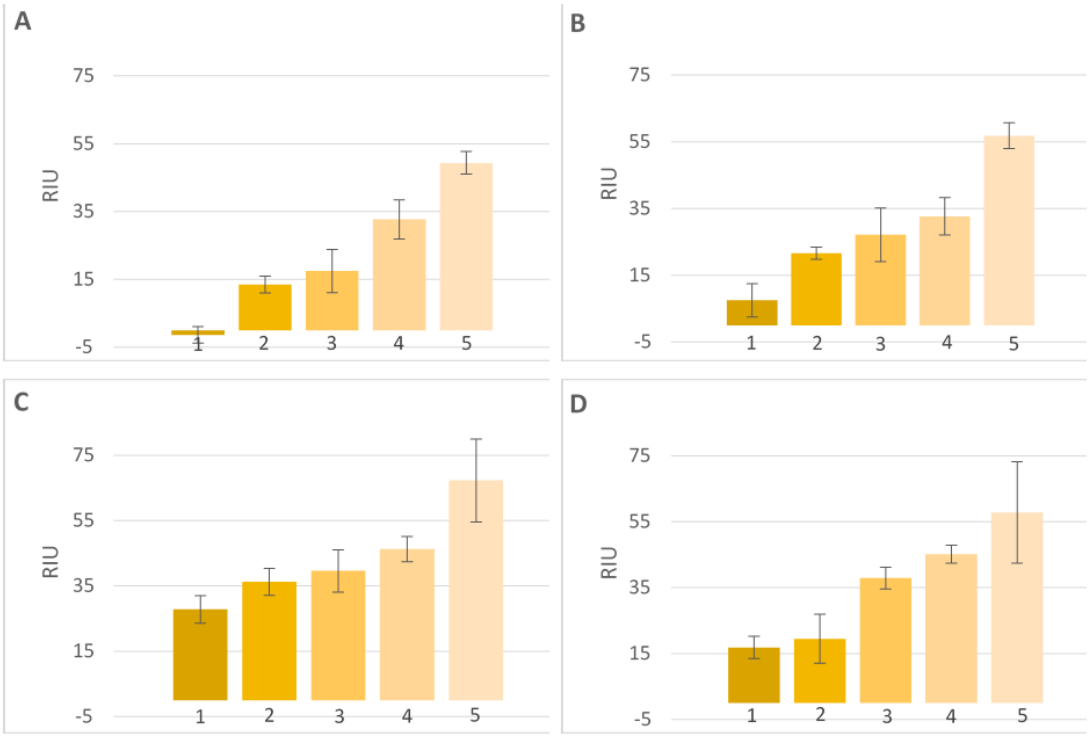

Figure 4.17: The effect of buffer composition on signal intensity recorded on Oleispira-specific sensor surfaces. Refractive index unit (RIU) values after 367 s (n=3, error bars show ± s.d.) for 1: Universal (Uni), 2: 2-mismatched Oleispira (MM2), 3: 1-mismatched Oleispira (MM1), 4: Oleispira oligo (Olei) and 5: positive control (REF, n=2). A: DPBS, B: DPBS-T (DPBS + 1% Tween-20), C: DPBS high salt (500 mM NaCl), D: DPBS-U (DPBS + 200 mM urea).

The Uni oligo, which is not complementary to sensor 4, yielded the lowest RIU value on the Oleispira specific sensor among the samples throughout all buffers (fig. 4.17). The lowest Uni was obtained in DPBS (A), while high salt DPBS (C) yielded the highest RIU values. The positive control (REF) yielded the highest RIU values in all buffer approaches among the samples. With high salt DPBS the highest values for REF were reached, while DPBS yielded the lowest among the buffers. What differentiated the buffers were slight differences between the perfect match and the MM1, the highest difference could be obtained in DPBS (fig. 4.17, A). The least difference between perfect match and MM1 was obtained in DPBS high salt and DPBS-T (B). The best discrimination between REF and MM2 could be observed in DPBS-U (D) and DPBS. The least difference between these two samples was obtained in high salt DPBS. The highest difference between Uni and perfect match were obtained in DPBS and the least in high salt DPBS.

The highest RIU values in general were observed with high salt DPBS, while the highest differences in RIU values among the samples were observed with the use of DPBS. The background signal increased with the use of Tween-20, higher salt concentrations and the use of urea, together with decreasing differences among the samples' RIU values.

4.7.2 Detection of combined oligos

Two amplification strategies were tested in order to confirm that binding of the target analyte was not inhibited in ESP compatible buffer solution. The experiments were conducted with a 24-nt long combined oligo, complementary to the Oleispira specific morpholino on sensor 3 and to the biotinylated universal oligo, which was used as signal amplification probe in combination with streptavidin coated magnetic beads.

Capture approach

As can be seen in figure 4.18, the combined oligo in ESP buffer (washed and injected in DPBS-T), yielded RIU values around 500. The RIU decreased after the flush step and stabilized within 2 min (tab. 3.12, fig. 4.18). As a positive control, the combined oligo was run with the sequential approach. Its values were almost twice as high as obtained with the capture approach (tab. 4.4).

Table 4.4: Average RIU values ($\pm$ s.d.) on Oleispira-specific sensor 3 with the capture approach. NTC: no-template control, biotinylated beads (n=3); combined oligo: 1 μM, blanked (n=3); positive control: combined oligo, 1 μM, blanked, run with sequential approach (n=1).

Sample	Average RIU ($\pm$ s.d.)
NTC	17.6 $\pm$ 3.75
combined oligo	461.8 $\pm$ 21
positive control	931.1

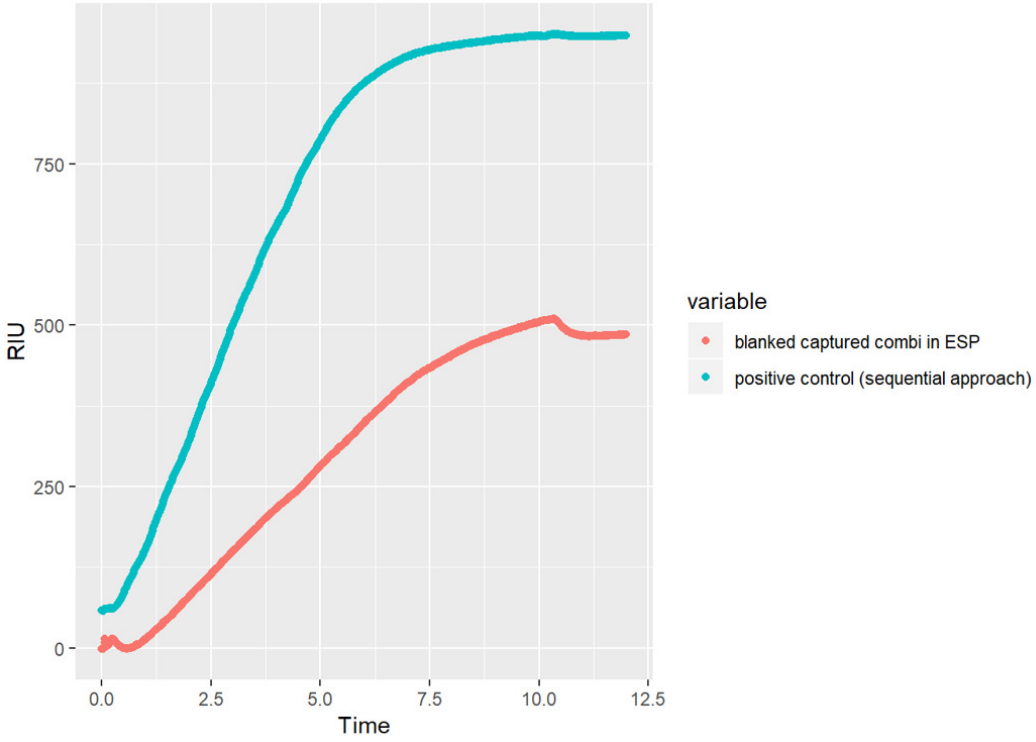

Figure 4.18: Obtained RIU values with the combined oligo in ESP buffer, washed and injected in DPBS-T, following the capture approach. A positive control (combined oligo 10 μM) was run following the sequential approach. The background was subtracted from values before plotting.

Sequential approach

To further confirm that ESP buffer could be used for the injection of the samples, the combined oligo was diluted in ESP (CE) and in a second approach also injected in ESP (CEE). As a positive control, the combined oligo in DPBS was injected in DPBS-T. The positive control (fig. 4.19, red) yielded the lowest RIU value. The signal on sensor 3 (Oleispira specific morpholino) increased with time and stabilized after approximately 7 min. CE and CEE had increasing RIU values within the first 10 min of measurements. Both showed an abrupt decrease in RIU after the flush step at approximately 10 min with a stabilization of the signal after 12 min. With CE the highest final RIU values (at the end of measurements) were obtained.

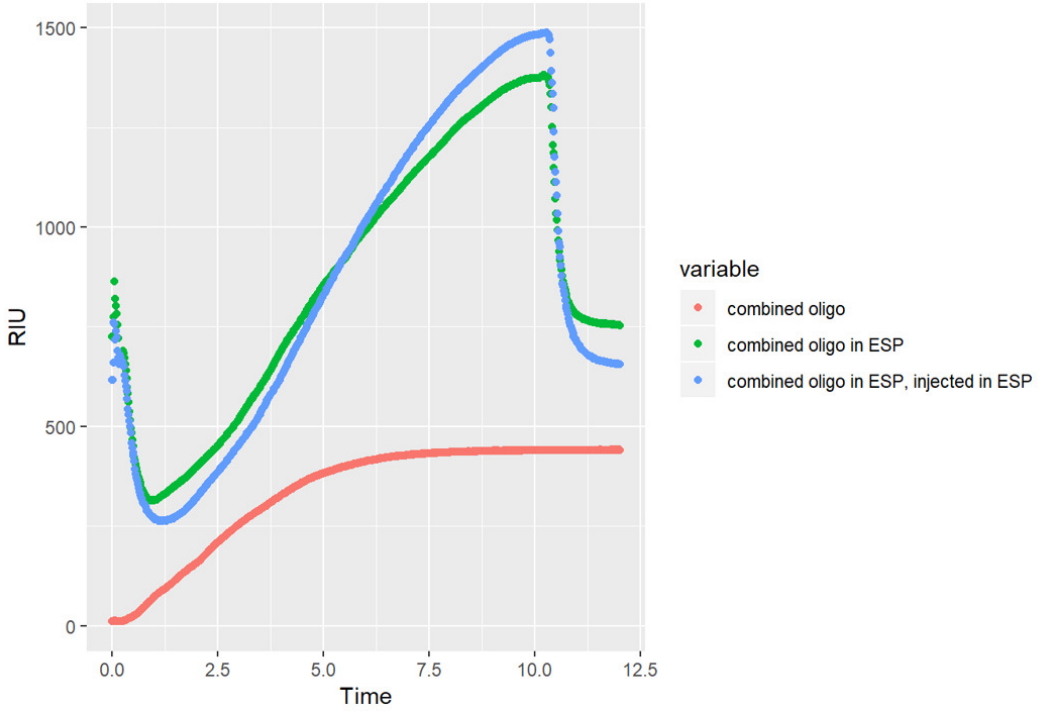

Figure 4.19: Obtained RIU values with combined oligos following the sequential approach. The combined oligo had a concentration of 1 uM. Red: positive control (combined oligo) in DPBS, injected in DPBS-T; Green: combined oligo in ESP, injected in DPBS-T (CE); Blue: combined oligo in ESP, injected in ESP (CEE). Background signal was subtracted from values before plotting.

4.7.3 Detection of PCR products

PCR products were generated from gene fragments mimicking the target 16S rRNA. The 477 bp PCR product (fig. 4.20, red) did not give a signal on the Oleispira specific sensor 3. The 90 bp products signal increased with time and gave a maximum signal around 30 units after 10 min. The positive control (blue) signal increased drastically until min 10, stabilized and reached a maximum value of 1200.

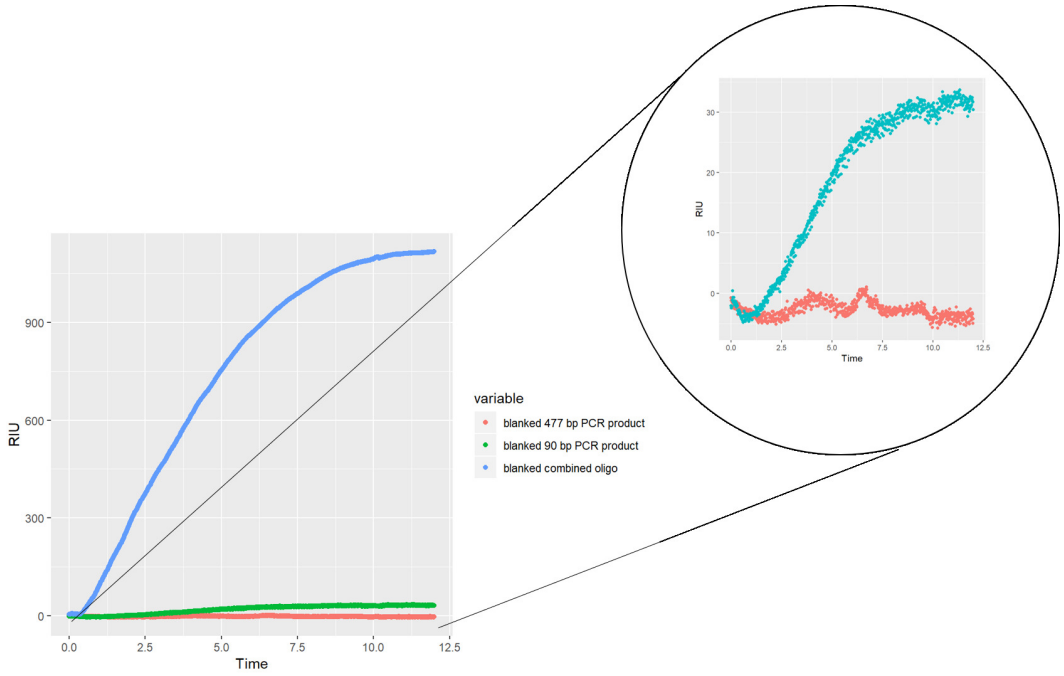

Figure 4.20: Obtained RIU values with 90 and 477 bp PCR product and combined oligo following the sequential approach. The combined oligo had a concentration of 1 uM. Red: 477 bp PCR product, injected in DPBS-T; Green: 90 bp PCR product, injected in DPBS-T; Blue: combined oligo in DPBS (0.5 nM), injected in DPBS-T. Background signal was subtracted from values before plotting

5 Discussion

Oleispira antarctica culture

Before starting the experiments, presence of *O. antarctica* cells in the cultivated cultures had to be confirmed. Rod-shaped cells were observed on the DAPI-stained microscope slides. However, the single flagellum, observed with electron microscopy by Yakimov et. al [92], could not be observed with this method. The growth of two *O. antarctica* cultures was compared at different temperatures. The culture grown at 4°C had a slower growth rate compared to the culture grown at 12°C. It needed twice as much time to enter the exponential phase and its maximum OD_{600} values were 2.5x lower. The optimal growth temperature of *O. antarctica* is between 1 to 15°C [24, 92]. Depending on the carbon-source, the growth of *O. antarctica* can differ with temperature [23]. Dilution experiments were conducted in order to determine the order of magnitude of the number of cells present in the liquid culture that was maintained. The blank, only containing media, started to show turbidity after day 10. It probably got contaminated with bacteria during the process of measuring OD_{600}, due to unwary pipetting technique. Since from the 10^{-8} culture on no growth was observed in the tubes, the 10^{-10} culture was seen reliable to further serve as blank. When observing the plots obtained with flow cytometry, two populations occured. As pointed out in the results, particles from stained FSW appeared to have the same size as *O. antarctica* cells, hence cells were discriminated according to fluorescence intensity. The left population, occurring in all samples, was mostly background noise (fig. 4.6, brown) from the stained FSW, which was subtracted from sample values. Events were counted when the fluorescence intensity was above the set threshold. The higher the nucleic acid content of a cell, the higher the fluorescence intensity. Low fluorescence intensity can occur when the cell is less active or damaged, while high intensity means that the cell is more active. Higher fluorescence intensity can also occur due to cell division. The obtained differences between the plate counting method and flow cytometry when estimating cell numbers were not expected. The values differed in one order of magnitude, the only possible reason for that could have been a mistake in preparing the dilution series, resulting in dilutions one order of magnitude higher or lower in one of the methods used.

RNA hybridization and capture experiments

The ESP is a stand-alone genosensor designed for autonomous collection of water samples and applied for *in situ* molecular probing. The final approach of this thesis was to establish a protocol for SPR analysis of *O. antarctica* and to implement the SPR module into the 3G ESP. Within the context of mimicking ESP conditions, several approaches have been tested to improve the capture of the target 16S rRNA out of a RNA pool. Four different hybridization buffers were tested, following experiments reported that have successfully been used to detect 16S rRNA with DNA probes [59, 62, 72]. According to Nelson et. al [62], no binding of the target 16S rRNA could be observed without the denaturation step (procedure G). The denaturation unfolded the secondary structure of the 16S RNA, making it fully single stranded (ss) and thereby making its target site more accessible for hybridization. 16S rRNA from *E. coli* in estimated concentrations of 2 nM had been successfully used by Nelson et. al [62]. Miyatake et. al [59] stated that increased content of denaturing agent, such as formamide, would result in higher sequence specificity. Hence, hybridization buffer with 0 and 25% of formamide were prepared and compared. Mimicking the reaction conditions in the ESP as outlined by Preston et. al [72], a GuSCN-based reagent, ESP buffer, was employed. This buffer is stated to effectively disrupt cells and inactivate nucleases, while at the same time allowing hybridizations at lower temperatures than with NaCl-based buffers [71]. Since all three articles reported positive results with capturing the 16S rRNA from RNA pools, it was expected to be able to reproduce these. The goal of the capture approach was to specifically enrich the target 16S rRNA. As can be seen from the obtained results, the capture approach had a very low capture efficiency, independent of the protocols used. The hybridization conditions were altered in order to assess the reason for the low efficiency.
In some probes fragments smaller than 100 bp could be observed. These appear most likely due to the biotinylated probe, which was given to the samples in a 50 to 100x excess. The captured control samples did not show any bands around the 500 and 800 bp mark, which states that the unspecific binding events with this approach were decreased to a minimum. The high molecular weighted band that appeared in some of the samples at the top of the gel is very likely to be beads pipetted onto the gel. A smear appeared below the 16S rRNA band in the captured test samples, while following the ESP and HBII protocol (fig. 4.13, lane 4, 5, 8, procedure D and F), caused by the degradation of the captured 16S rRNA. Another reason for the smear could be the change of the elution step from 3 min at 90°C to 5 min at 95°C. The band below 100 bp mark is, as previously stated, very likely to be the biotinylated probe. In this capture approach (fig. 4.13) a different type of magnetic beads was used (M-270). 25 μL of these beads (M-270) were given to the samples, capable of binding 50 pmol of ss oligonucleotides. The biotinylated probe itself was 50 pmol, while the overall 16S rRNA content was 250 ng which corresponds to 0.5 pmol. The biotinylated probe might bind faster to the beads, since it is much smaller than the

16S rRNA. Using a lower extent of probe to sample (e.g. probe concentration of 12.5 pmol, 25x extent of target 16S rRNA), seems to be promising in terms of reducing the binding of unhybridized probe to the streptavidin molecules on the surface of the beads. Furthermore, the binding of the ~1500 bp 16S rRNA molecule might cover binding sites on the beads due to its size as well as negatively repelling other molecules and thus preventing or exacerbating binding [82]. Therefore, it might be that the binding of 16S rRNA and non-hybridized biotinylated probe have saturated the beads, leaving leftover unbound biotinylated probe. The secondary structure of the 16S rRNA makes it challenging to detect, since hybridization kinetics are slowed down, and the sequences accessibility is decreased [62]. The position of the capture sequence in the 16S rRNA of *O. antarctica* (fig. 5.1), which seems to be difficult to access, could have hampered its binding and caused an insufficient capture of the target out of the RNA pool.
In some of the performed experiments the 16S rRNA content was too low to give reliable results with Nanodrop. This demands the need to improve the capture conditions in terms of the hybridization buffer and the beads used as well as the protocol for the hybridization.

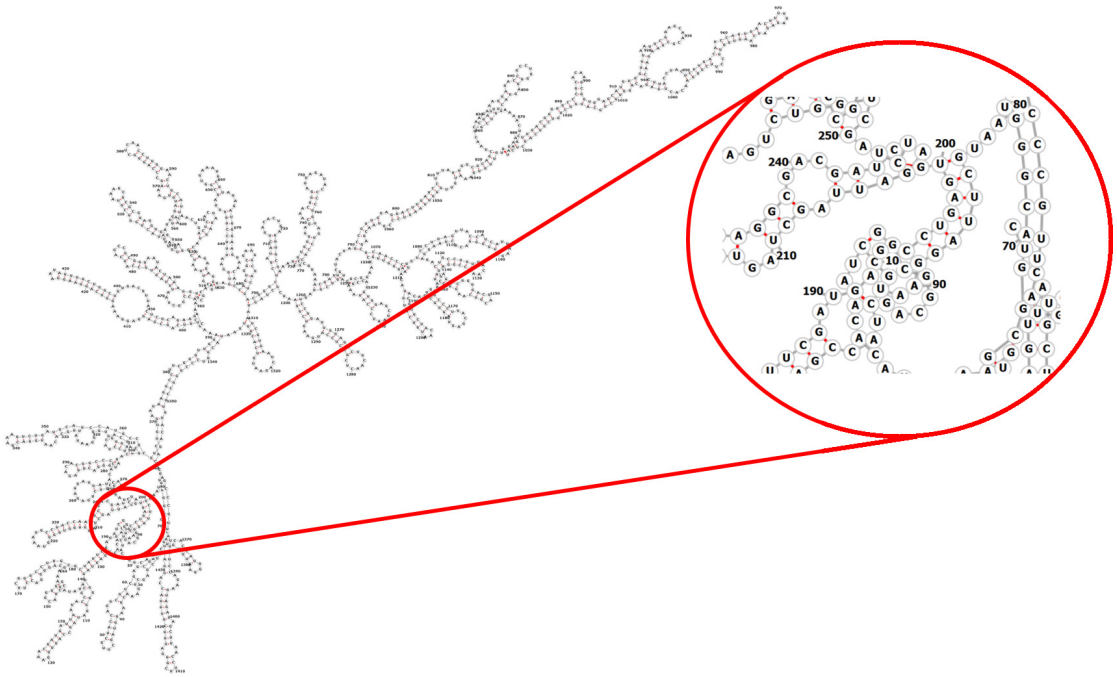

Figure 5.1: Predicted secondary structure of *O. antarctica* obtained from [86]. The highlighted region shows the sequence complementary to the capture (biotinylated universal) probe.

SPR experiments

Specificity testing

One of the major advantages of morpholino based probes towards DNA based probe is the decreased sensitivity to buffer composition such as insensitivity to ionic strength [45]. SPR is well established for DNA-DNA binding [6, 82]. Sipova et. al [82] have stated that decreased salt content or use of denaturing agents enhance the sequence specificity. Sequence specificity on the sensors can be seen as the ability of discriminating MM1 and MM2 oligos from the perfect match. Less specificity would mean increased probability of false-positives, indicating that Oleispira is present in the sample even though it might not be. The importance of discriminating one or two mismatches can be seen with the use of the ProbeMatch tool (Silva database), a web application to check the specificity of primers, when comparing sequences that allow mismatches to sequences that allow no mismatch at all. Using the Oleispira-specific probe and allowing no mismatches, only hits for *O. antarctica* and *O. lenta* and non-cultured *Oceanospirillales* can be found. While, when allowing MM1, the database has 365 hits from *Marinomonas* to *Thalassolituus* and when allowing MM2 the database search results in over 3000 hits ranging from *Neptuniibacter* and *Ferrimonas* to *Cabdidatus* and *Dasania*. Nonetheless, organisms with only one or two mismatches in the specified region can be physiologically and functionally closely related to Oleispira and other marine oil-degrading bacteria.
With decreasing mismatch number, the signal intensity increased on the Oleispira-specific sensor. This trend could be observed with all buffers tested. The background signal increased in all other buffers than DPBS, meanwhile the differences among the samples' RIU values decreased. High standard deviations were obtained with samples ran in high salt DPBS and DPBS-U. The lower the mismatch number, the more specific is the binding of the sample to the detection probe. The more specific and sensitive the sensors are towards the target probe, the higher the discrimination among the mismatched samples compared to the perfectly matching sample. The best results, i.e. highest discrimination of mismatched samples compared to perfectly matching samples, were obtained in DPBS buffer. The high standard deviations obtained with DPBS high salt and DPBS-U are probably due to decreasing sensor specificity. Unspecific binding events occurred with usage of DPBS-T. Tween-20 is primarily used for preventing hydrophobic interactions [63], the occurring unspecific binding events are deductively charge-based. A lower concentration of salt in the high salt DPBS, e.g. using concentrations of NaCl of 200 or 300 mM instead of 500 mM, could have resulted in less unspecific binding. Due to the restricted time schedule of this thesis this was not further investigated.

Amplification strategies

It is planned to implement capture of bacterial rRNA, based on the separation of magnetic beads, into the SPR system [6]. Two different hybridization strategies, as described earlier and pointed out in [17], were carried out with the combined oligo, complementary to the Oleispira specific probe. Both strategies were successful in terms of signal amplification. The indirect capture (hybridizing probe and sample, then adding the beads) has shown to yield lower results than the sequential approach, in which probe and sample are hybridized and injected, followed by a bead injection [6, 17]. This could be replicated with the experiments conducted in this study. Hence, the sequential approach was further used for SPR detection experiments. PCR products, generated from gene fragments that were mimicking the target 16S rRNA, were used to observe the potential of the developed method to detect longer molecules in ESP buffer. The experiment conducted showed the need to further improve the protocol for capturing longer molecules, as the 477 bp PCR product yielded signals below the background noise and the 90 bp PCR product only slightly above it, compared to excellent signal with the combined oligo. One reason for the low signal response on the sensors could have been too low concentrations of the PCR products or fragmentation during the denaturing step, making it difficult to detect the target molecule.

6 Conclusion

The goal of this study was to develop an SPR based genosensor to be implemented into the 3G ESP. Due to the scope of this thesis and drawbacks within the conduction of experiments, this could not be entirely reached. The RNA extraction with ESP buffer was comparable to commercially available extraction methods and showed the potential to be used for RNA extraction in future experiments. The different hybridization buffers and protocols used, had a very low capture efficiency and results obtained by others, following the same procedures, could not be reproduced. Among the hybridization buffers used, experiments with HBII buffer were the most promising, yielding a visible band of the target 16S rRNA, yet with still very low concentrations. A 50x excess of biotinylated probe compared to the RNA content yielded acceptable results. In terms of the sensors specificity, best results were obtained in DPBS buffer. The use of high salt concentrations and denaturing agents resulted in less specific signals on the sensors. As shown in earlier publications and shown in this study, the sequential signal amplification approach yielded better results than the capture approach. The sequential approach yielded excellent results with the combined oligos, while the usage of PCR fragments resulted in poor signals on the sensors. This demands for further studies on the detection of longer molecules before applying this method to detect bacteria in the marine environment.

7 Future Perspectives

Several possibilities exist to further improve the SPR system. Since the SPR sequential approach with ESP buffer has proven to work for combined oligos it has the potential to work for RNA. Starting with longer molecules, a method should be developed to detect longer single stranded DNA fragments, like the generated 90 and 477 bp PCR products or to *in vitro* synthesize RNA. As detection probes, alternatives to nucleic acids (NA) such as LNA [87] and PNA have been used. PNA have been found to have a higher binding affinity towards NA [36, 85] and are therefore specifically used in hybridization approaches [80]. The use of metal nanoparticles such as gold nanoparticles seem to be promising for signal amplification. LODs as low as 1 pM have been reported in a similar approach with surface plasmon resonance imaging (SPRi) [46]. An interesting approach was also reported by Guner et. al [28], where they used a smartphone-based SPRi system. This system is very cost-efficient meanwhile being easy portable, yet not yielding as low LODs as the system used here.
Molecularly imprinted polymers (MIP), robust plastic antibodies with increased chemical and physical stability [69], have been found to yield low LODs. Yilmaz and coworkers [94] used atrazine imprinted nanoparticles for pesticide detection with a LOD of 0.7 ng/mL. In another approach a macroporous molecularly imprinted film was used for the detection of testosterone in PBS with a femtomolar detection limit, so far among the lowest values reported [96]. Instead of targeting bacterial nucleic acids, the detection of PAHs in the marine environment could be an alternative, since previous reports have proven to detect these at fairly low concentrations.

Appendix

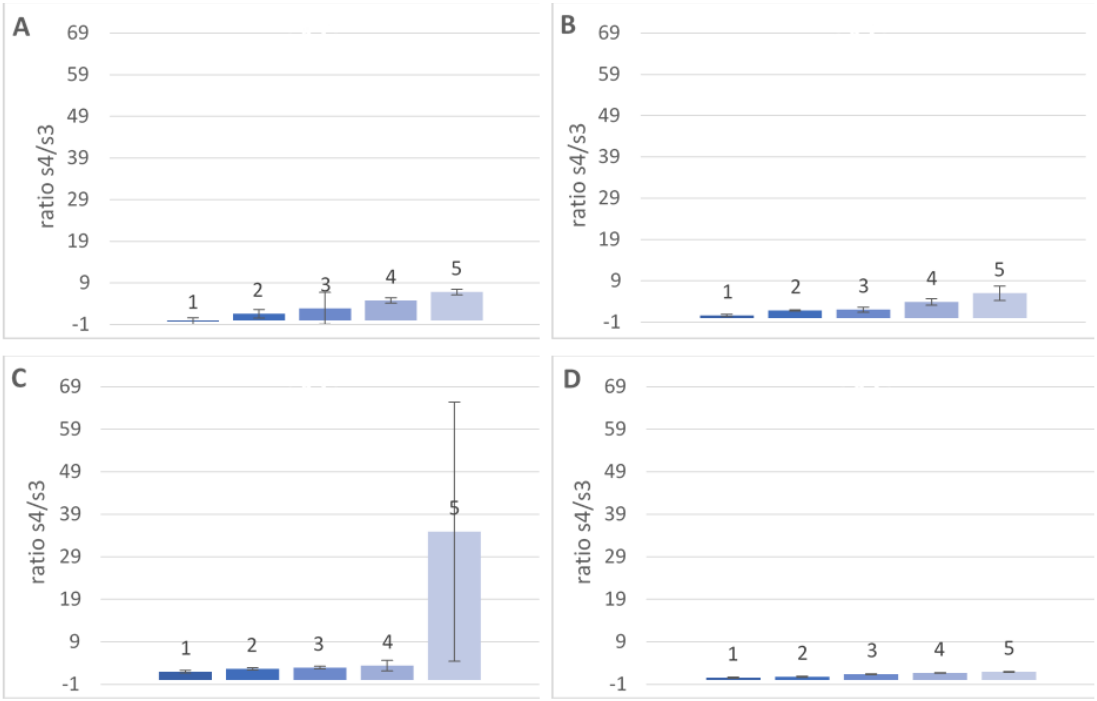

Figure 1: Average ratio of sensor 4 (Oleispira) to sensor 3 (control) with standard deviation for Universal (1), 2-mismatched Oleispira (2), 1-mismatched Oleispira (3), Oleispira oligo (4) and the positive control (5). n=3 except for positive control (n=2). A: DPBS, B: DPBS-T (DPBS + 1% Tween-20), C: DPBS high salt (500 mM NaCl), D: DPBS-U (DPBS + 200 mM urea); s4: sensor 4; s3: sensor 3.

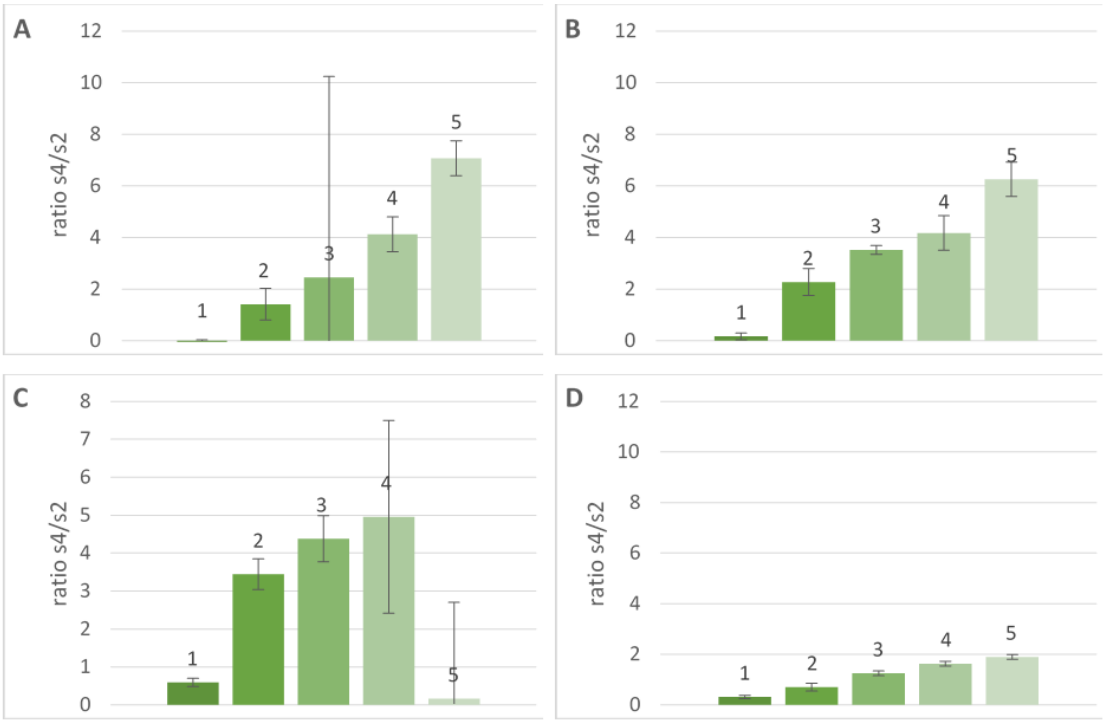

Figure 2: Average ratio of sensor 4 (Oleispira) to sensor 2 (Universal) with standard deviation for Universal (1), 2-mismatched Oleispira (2), 1-mismatched Oleispira (3), Oleispira oligo (4) and the positive control (5). n=3 except for positive control (n=2). A: DPBS, B: DPBS-T (DPBS + 1% Tween-20), C: DPBS high salt (500 mM NaCl), D: DPBS-U (DPBS + 200 mM urea); s4: sensor 4; s2: sensor 2.

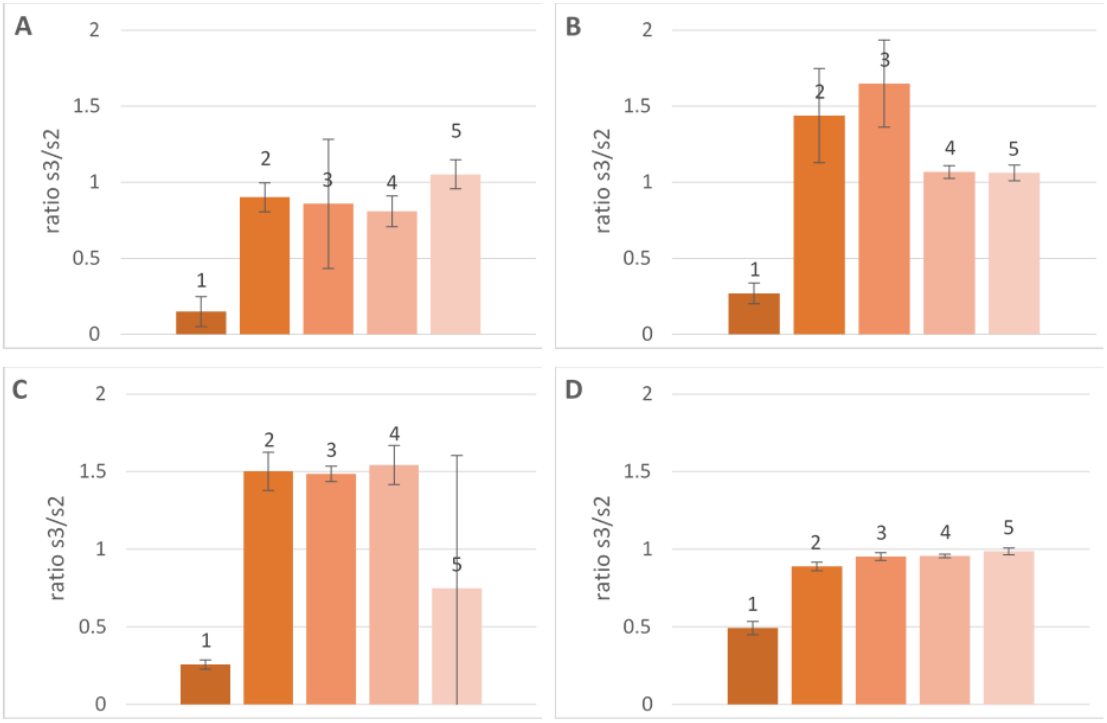

Figure 3: Average ratio of sensor 3 (control) to sensor 2 (Universal) with standard deviation for Universal (1), 2-mismatched Oleispira (2), 1-mismatched Oleispira (3), Oleispira oligo (4) and the positive control (5). n=3 except for positive control (n=2). A: DPBS, B: DPBS-T (DPBS + 1% Tween-20), C: DPBS high salt (500 mM NaCl), D: DPBS-U (DPBS + 200 mM urea); s3: sensor 3; s2: sensor 2.

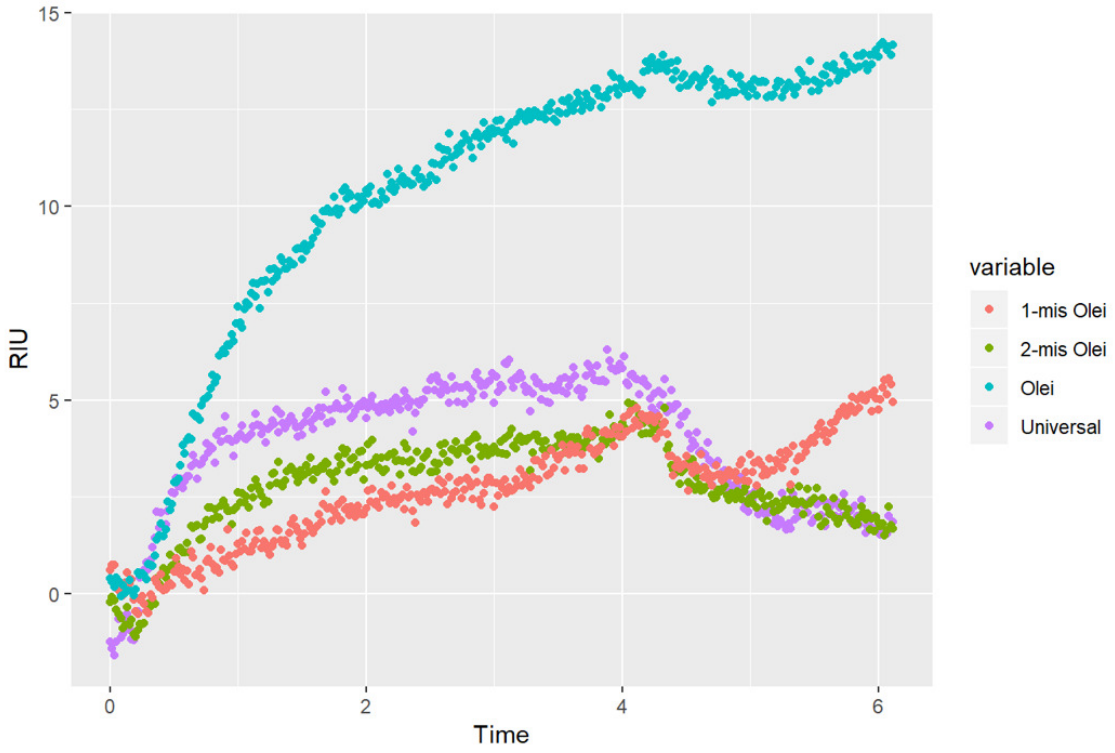

Figure 4: RIU values of one replicate of Uni, 2MM, 1MM and Olei for 2x diluted DPBS plotted against time. Shown are only the measured signals on sensor 4.

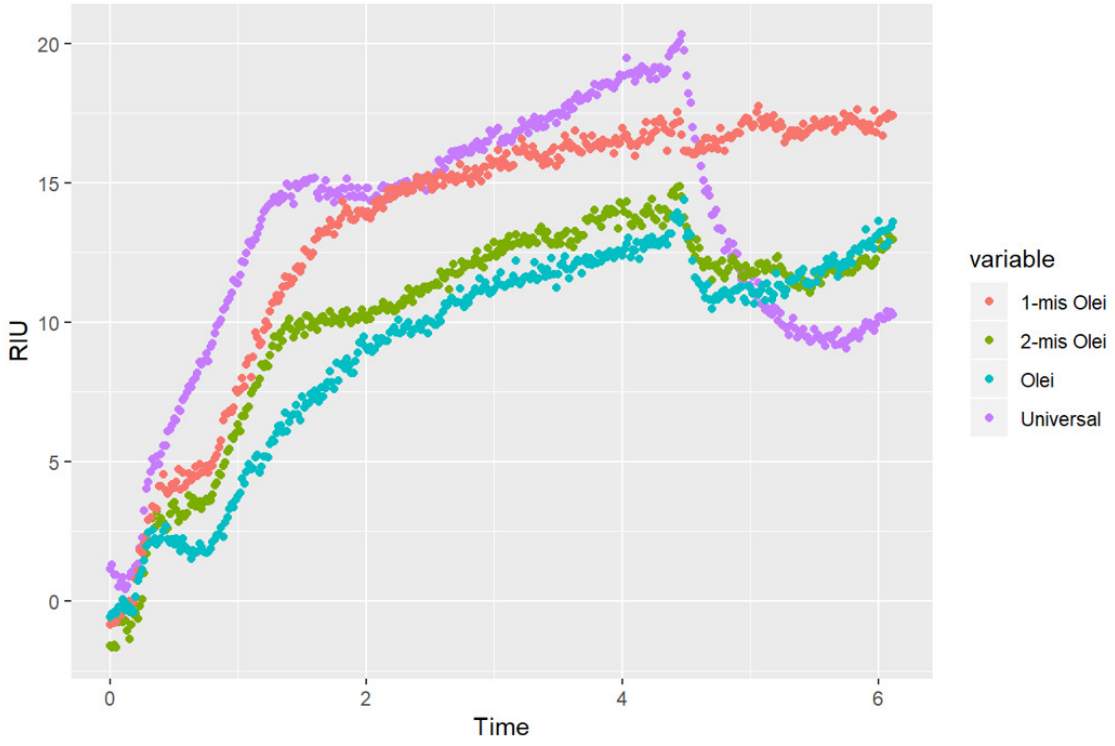

Figure 5: RIU values of one replicate of Uni, 2MM, 1MM and Olei for 10x diluted DPBS. Shown are only the measured signals on sensor 4.

Table 1: Nanodrop determined concentrations of the RNA capture approach with HBI and 10 min incubation at 70°C, followed by 20 min incubation at RT.

sample	type	code	conc. ($ng/\mu L$)
start RNA-1	starting material	RNA-01	317.0
start RNA-2	starting material	RNA-02	
unbound RNA-1	test	UB RNA-1	323.1
unbound RNA-2	test	UB RNA-2	318.9
unbound RNA-3	control	UB RNA-3	312.4
unbound RNA-4	control	UB RNA-4	289.4
captured RNA-1	test	CP RNA-1	5.5
captured RNA-2	test	CP RNA-2	4.5
captured RNA-3	control	CP RNA-3	3.6
captured RNA-4	control	CP RNA-4	1.0

Table 2: Nanodrop determined concentrations for the RNA capture approach with ESP (10 min at 100°C, followed by 30 min at 27°C) and HBI (10 min at 70°C, 30 min at RT and incubation overnight at RT on a rotator).

sample	type	code	conc. ($ng/\mu L$)
start RNA-0	starting material	RNA-0	43.2
unbound RNA1 in ESP	test	U ESP1	37.5
unbound RNA2 in ESP	test	U ESP2	33.8
unbound RNA3 in ESP	control	U ESP3	39.6
unbound RNA4 in ESP	control	U ESP4	33.9
captured RNA1 in ESP	test	C ESP1	21.5
captured RNA2 in ESP	test	C ESP2	22.6
captured RNA3 in ESP	control	C ESP3	9.4
captured RNA4 in ESP	control	C ESP4	11.8
unbound RNA1 in HB	test	U HB1	40.0
unbound RNA2 in HB	test	U HB2	39.3
unbound RNA3 in HB	control	U HB3	37.8
unbound RNA4 in HB	control	U HB4	39.6
captured RNA1 in HB	test	C HB1	9.0
captured RNA2 in HB	test	C HB2	17.3
captured RNA3 in HB	control	C HB3	6.4
captured RNA4 in HB	control	C HB4	8.3

Table 3: Nanodrop determined concentrations for the RNA capture approach with HBII (10 min at 70°C, 30 min at RT and overnight incubation on a rotator) and HBU (10 min at 100°C, followed by 30 min at 27°C).

sample	type	code	conc. ($ng/\mu L$)
uncleaned RNA	extracted RNA	Olei extr	236.1
extracted Olei RNA	starting material	RNA 4	179.3
unbound RNA1 in HBII	test	U HBII1	29.0
unbound RNA2 in HBII	test	U HBII2	31.6
unbound RNA3 in HBII	control	U HBII3	31.0
unbound RNA4 in HBII	control	U HBII4	40.3
captured RNA1 in HBII	test	C HBII1	20.2
captured RNA2 in HBII	test	C HBII2	20.1
captured RNA3 in HBII	control	C HBII3	5.4
captured RNA4 in HBII	control	C HBII4	9.9
unbound RNA1 in HBU	test	U HBU1	19.8
unbound RNA2 in HBU	test	U HBU2	27.4
unbound RNA3 in HBU	control	U HBU3	28.0
unbound RNA4 in HBU	control	U HBU4	22.5
captured RNA1 in HBU	test	C HBU1	17.3
captured RNA2 in HBU	test	C HBU2	8.1
captured RNA3 in HBU	control	C HBU3	7.7
captured RNA4 in HBU	control	C HBU4	6.1

Table 4: Nanodrop determined concentrations of the RNA capture approach with HBII (5 min at 65°C, followed by 15 min at RT) and ESP (5 min at 85°C, followed by 10 min at RT).

sample	type	code	conc. ($ng/\mu L$)
extracted Olei RNA	starting material	RNA 1	175.2
extracted Olei RNA	starting material	RNA 4	179.3
captured RNA1 in HBII	test	C HBII1	11.4
captured RNA2 in HBII	test	C HBII2	26.1
captured RNA3 in HBII	control	C HBII3	3.0
captured RNA4 in HBII	control	C HBII4	3.9
captured RNA1 in ESP	test	C ESP1	23.7
captured RNA2 in ESP	test	C ESP2	26.4
captured RNA3 in ESP	control	C ESP3	10.6
captured RNA4 in ESP	control	C ESP4	9.8

Table 5: Nanodrop determined concentrations of the RNA capture approach with HBII (5 min at 65°C, followed by 15 min at RT) and ESP (5 min at 85°C, followed by 10 min at RT).

sample	type	code	conc. ($ng/\mu L$)
extracted Olei RNA	starting material	RNA 2	166.18
captured RNA1 in HBII	test	C HBII1	11.47
captured RNA2 in HBII	test	C HBII2	23.95
captured RNA3 in HBII	control	C HBII3	3.84
captured RNA4 in HBII	control	C HBII4	6.02
captured RNA1 in ESP	test	C ESP1	11.09
captured RNA2 in ESP	test	C ESP2	10.33
captured RNA3 in ESP	control	C ESP3	6.52
captured RNA4 in ESP	control	C ESP4	1.59

Table 6: Nanodrop determined concentrations for the RNA double bead capture approach with HBII (5 min at 65°C, 15 min at room temperature) with a probe concentration of 2.5 pmol.

sample	type	code	conc. ($ng/\mu L$)
captured RNA1 in HBII	test	C HBII 1	1.10
captured RNA2 in HBII	test	C HBII 2	3.81
captured RNA3 in HBII	control	C HBII 3	0.64
captured RNA4 in HBII	control	C HBII 4	0.39
captured RNAI in HBII	test	C HBII I	4.25
captured RNAII in HBII	test	C HBII II	3.36
captured RNAIII in HBII	control	C HBII III	1.08
captured RNAIV in HBII	control	C HBII IV	1.37

Table 7: Nanodrop determined concentrations for the RNA capture approach with ESP (5 min at 85°C, 10 min at room temperature) and HBII (10 min at 65°C, followed by 15 min at room temperature) and a probe concentration of 2.5 pmol.

sample	type	code	conc. ($ng/\mu L$)
captured RNA1 in ESP	test	C ESP 1	12.05
captured RNA2 in ESP	test	C ESP 2	15.55
captured RNA3 in ESP	control	C ESP 3	23.21
captured RNA4 in ESP	control	C ESP 4	10.17
captured RNAI in ESP	test	C ESP I	8.32
captured RNAII in ESP	test	C ESP II	6.72
captured RNAIII in ESP	control	C ESP III	7.89
captured RNAIV in ESP	control	C ESP IV	7.19
captured RNA1 in HBII	test	C HBII 1	4.30
captured RNA2 in HBII	test	C HBII 2	4.48
captured RNA3 in HBII	control	C HBII 3	0.58
captured RNA4 in HBII	control	C HBII 4	2.71
captured RNAI in HBII	test	C HBII I	2.54
captured RNAII in HBII	test	C HBII II	3.92
captured RNAIII in HBII	control	C HBII III	2.60
captured RNAIV in HBII	control	C HBII IV	4.47

Table 8: Nanodrop determined concentrations of extracted DNA and RNA of *O. antarctica* with Zymo BIOMICS.

sample	conc. ($ng/\mu L$)
Olei DNA 1	20.59
Olei DNA 2	22.75
Olei DNA 3	17.11
Olei DNA 4	17.02
Olei RNA 1	78.71
Olei RNA 2	85.94
Olei RNA 3	77.35
Olei RNA 4	71.75

Oleispira rRNA sequence

- blue: Oleispira oligo
- red: Universal probe

DNA sequence (forward)

```
   1 GGCGGCAGGC CTAACACATG CAAGTCGAGC GGAAACGAAG GTAGCTTGCT ACCAGGCGTC
  61 GAGCGGCGGA CGGGTGAGTA ATGCTTAGGA ATCTACCGAG TAGTGGGGGA TAGCCATTGG
 121 AAACGATGAT TAATACCGCA TATATCCTAC GGGGGAAAGC AGGGGACCTT CGGGCCTTGC
 181 GCTATTCGAT GAGCCTGAGT GAGATTAGCT AGTTGGTGGG GTAAAGGCCT ACCAAGGCGA
 241 CGATCTCTAG CTGGTCTGAG AGGATGATCA GCCACACTGG GACTGAGACA CGGCCCAGAC
 301 TCCTACGGGA GGCAGCAGTG GGGAATATTG CACAATGGAC GAAAGTCTGA TGCAGCCATG
 361 CCGCGTGTGT GAAGAAGGCC TTCGGGTTGT AAAGCACTTT CAGCGAGGAG GAAAGGTCAG
 421 TAAGTAATAT TTGCTGGCTG TGACGTTACT CGCAGAAGAA GCACCGGCTA ATTTAGTGCC
 481 AGCAGCCGCG GTAATACTAA AGGTGCAAGC GTTAATCGGA ATTACTGGGC GTAAAGCGCG
 541 CGTAGGTGGT TTGTTAAGTT GGATGTGAAA GCCCAGGGCT CAACCTTGGA ACTGCATTCA
 601 AAACTGACTC ACTAGAGTAC GAGAGAGGTT AGTGGAATTT CCTGTGTAGC GGTGAAATGC
 661 GTAGAGATGG GAAGGAACAC CAGTGGCGAA GGCGACTGAC TGGCTCGATA CTGACACTGA
 721 GGTGCGAAAG CGTGGGGAGC AAACGGGATT AGATACCCCG GTAGTCCACG CCGTAAACGA
 781 TGTCTACTAG CCGTTGGAGG ACTTGATCCT TTAGTGGCGC AGCTAACGCG ATAAGTAGAC
 841 CGCCTGGGGA GTACGGTCGC AAGATTAAAA CTCAAATGAA TTGACGGGGG CCCGCACAAG
 901 CGGTGGAGCA TGTGGTTTAA TTCGAAGCAA CGCGAAGAAC CTTACCTACT CTTGACATCC
 961 AGTGAACTTT TGAGAGATCA ATTGGTGCCT TCGGGAACAC TGAGACAGGT GCTGCATGGC
1021 TGTCGTCAGC TCGTGTTGTG AAATGTTGGG TTAAGTCCCG TAACGAGCGC AACCCTTGTC
1081 CTTAGTTACC ATCATTAAGT TGGGGACTCT AAGGAGACTG CCGGTGACAA ACCGGAGGAA
1141 GGCGGGGACG ACGTCAAGTC ATCATGGCCC TTACGAGTAG GGCTACACAC GTGCTACAAT
1201 GGCATGTACA AAGGGTTGCC AAGCCGCGAG GTGGAGCTAA TCCCATAAAG CATGTCGTAG
1261 TCCGGATTGG AGTCTGCAAC TCGACTCCAT GAAGTCGGAA TCGCTAGTAA TCGTGAATCA
1321 GAATGTCACG GTGAATACGT TCCCGGGCCT TGTACACACC GCCCGTCACA CCATGGGAGT
1381 GGGTTGCTCC AGAAGTAGAT AGCTTAACCT TCGGGAGGGC GTTTACCAGG AGTATTC
```

Gene fragments

DNA sequence (Oleispira 477 bp)

```
   1 ATGAGCCTGA GTGAGATTAG CTAGTTGGTG GGGTAAAGGC CTACCAAGGC GACGATCTCT
  61 AGCTGGTCTG AGAGGATGAT CAGCCACACT GGGACTGAGA CACGGCCCAG ACTCCTACGG
 121 GAGGCAGCAG TGGGGAATAT TGCACAATGG ACGAAAGTCT GATGCAGCCA TGCCGCGTGT
 181 GTGAAGAAGG CCTTCGGGTT GTAAAGCACT TTCAGCGAGG AGGAAAGGTC AGTAAGTAAT
 241 ATTTGCTGGC TGTGACGTTA CTCGCAGAAG AAGCACCGGC TAATTTAGTG CCAGCAGCCG
 301 CGGTAATACT AAAGGTGCAA GCGTTAATCG GAATTACTGG GCGTAAAGCG CGCGTAGGTG
 361 GTTTGTTAAG TTGGATGTGA AAGCCCAGGG CTCAACCTTG GAACTGCATT CAAAACTGAC
 421 TCACTAGAGT ACGAGAGAGG TTAGTGGAAT TTCCTGTGTA GCGGTGAAAT GCGTAGA
```

DNA sequence (Oleispira 90 bp)

```
  1 ATGAGCCTGA GTGAGATTAG CTAGTTGGTG ATGTAAAGGC CTACCAAGGC GACGATCTCT
 61 AGCTGGTCTT GTAGCGGTGA AATGCGTAGA
```

Bibliography

[1] F. Abbasian et al. "A Comprehensive Review of Aliphatic Hydrocarbon Biodegradation by Bacteria". In: *Appl Biochem Biotech* 176 (2015), pp. 670–699. DOI: 10.1007/s12010-015-1603-5.

[2] R. Almeda et al. "Ingestion and sublethal effects of physically and chemicallydispersed crude oil on marine planktonic copepods". In: *Ecotoxicology* 23 (2014), pp. 988–1003. DOI: 10.1007/s10646-014-1242-6.

[3] D. M. Anderson et al. "Identification and enumeration of Alexandrium spp. from the Gulf of Maine using molecular probes". In: *Deep Sea Research Part II (Elsevier)* 52 (2005), pp. 2467–2490. DOI: 10.1016/j.dsr2.2005.06.015.

[4] AOAC. *Final report and executive summaries from the AOAC International Presidental Task Force on Best Price in Microbiological Methodology*. Report. AOAC Intenational, 2006.

[5] A. Baeumner. "Biosensors for environmental pollutants and food contaminants". In: *Analytical and Bioanalytical Chemistry* 377 (2003), pp. 434–445. DOI: 10.1007/s00216-003-2158-9.

[6] Andrea Bagi et al. "Implementing Morpholino-Based Nucleic Acid Sensing on a Portable Surface Plasmon Resonance Instrument for Future Application in Environmental Monitoring". In: *Sensors* 18.10 (2018). DOI: 10.3390/s18103259.

[7] Andrea Bagi et al. "Naphthalene biodegradation in temperate and arctic marine microcosms". In: *Biodegradation* 25.1 (2014), pp. 111–125. ISSN: 1572-9729. DOI: 10.1007/s10532-013-9644-3. URL: https://doi.org/10.1007/s10532-013-9644-3.

[8] BAM. *US Food and Drug Administration: Bacterial Analytical Manual*. Webpage. 2019. URL: https://www.fda.gov/food/laboratory-methods-food/bacteriological-analytical-manual-bam.

[9] T. Baussant. "Exploring novel DNA-based autonomous platform for marine water monitoring: Opportunities for petroleum and aquaculture industry". In: *Innovative vannovervakingsmetoder*. Vann, 2017, pp. 250–252.

[10] BDBioscience. *Threshold and Analysis of Small Particles on the BD Accuri C6 Cytometer*. Tech. rep. BD Bioscience, 2012.

[11] N. J. Borys, E. Shafran, and J. M. Lupton. "Surface plasmon delocalization in silver nanoparticle aggregates revealed by subdiffraction supercontinuum hot spots". In: *Scientific Reports (Nature)* 3.2090 (2013). DOI: 10.1038/srep02090.

[12] O. G. Brakstad, T. Nordtug, and M. Throne-Holst. "Biodegradation of dispersed Macondo oil in seawater at low temperature and different oil droplet sizes". In: *Marine Pollution Bulletin* 93 (2015), pp. 144–152.

[13] R. J. W. Brooijmans, M. I. Pastink, and R. J. Siezen. "Hydrocarbon-degrading bacteria: the oil-spill clean-up crew". In: *Microbial Biotechnology* 2.6 (2009), pp. 587–594. DOI: 10.1111/j.1751-7915.2009.00151.

[14] Edward Buskey, Helen White, and Andrew Esbaugh. "Impact of Oil Spills on Marine Life in the Gulf of Mexico: Effects on Plankton, Nekton, and Deep-Sea Benthos". In: *Oceanography* 29 (Sept. 2016), pp. 174–181. DOI: 10.5670/oceanog.2016.81.

[15] Tom Coenye and Peter Vandamme. "Intragenomic heterogeneity between multiple 16S ribosomalRNA operons in sequenced bacterial genomes". In: *FEMS Microbiology Letters (Elsevier)* 228 (2003), pp. 45–49. DOI: 10.1016/S0378-1097(03)00717-1.

[16] F. Coulon et al. "Effects of temperature and biostimulation on oil-degrading microbial communities in temperate estuarine waters". In: *Environmental Microbiology* 9.1 (2007), pp. 177–186.

[17] E. Da-Silva, L. Barthelmebs, and J. Baudart. "Development of a PCR-free DNA-based assay for the specific detection of Vibrio species in environmental samples by targeting the 16S rRNA". In: *Environmental Science and Pollution Research* 24 (2017), pp. 5690–5700. DOI: 10.1007/s11356-016-8193-9.

[18] K. DeAngelis et al. "PCR Amplification-Independent Methods for Detection of Microbial Communities by the High-Density Microarray PhyloChip". In: *Applied and Environmental Microbiology* 77.18 (2011), pp. 6313–6322. DOI: 10.1128/AEM.05262-11.

[19] DUBartholomew. *Spreeta Diagram and Sensors*. Accessed 2018-12-05. 2012. URL: https://commons.wikimedia.org/wiki/File:Spreeta_Diagram_and_Sensors(1).jpg.

[20] V. Ebenezer, L. K. Medlin, and J. ki. "Molecular Detection, Quantification, and Diversity Evaluation of Microalgae". In: *Marine Biotechnology (Springer)* 14.2 (2011), pp. 129–142. DOI: 10.1007/s10126-011-9427-y.

[21] European Space Agency. *Oil pollution monitoring*. URL: http://www.esa.int/esapub/br/br128/br128_1.pdf.

[22] A. M. Foudeh et al. "Rapid and specific SPRi detection of L. pneumophilain complex environmental water samples". In: *Analytical and Bioanalytical Chemistry (Springer)* 407 (2014), pp. 5541–5545. DOI: 10.1007/s00216-015-8726-y.

[23] G. Gentile et al. "Biodegradation potentiality of psychrophilic bacterial strain Oleispira antarctica RB-8T". In: *Marine Pollution Bulletin* 105.1 (2016), pp. 125–130. ISSN: 0025-326X. DOI: https://doi.org/10.1016/j.marpolbul.2016.02.041. URL: http://www.sciencedirect.com/science/article/pii/S0025326X16300972.

[24] P. N. Golyshin et al. *Oleispira: in Handbook of Hydrocarbon and Lipid Microbiology*. Ed. by K. N. Timmis. Springer, Berlin, Heidelberg, 2010. ISBN: 978-3-540-77584-3. DOI: 10.1007/978-3-540-77587-4_125.

[25] E. Gontikaki et al. "Hydrocarbon-degrading bacteria in deep-water subarcticsediments (Faroe-Shetland Channel)". In: *Journal of Applied Microbiology* 125 (2018), pp. 1040–1053. DOI: 10.1111/jam.14030.

[26] R. Govindarajan et al. "Microarray and its applications". In: *Journal of pharmacy & bioallied sciences* 4.2 (2012), pp. 310–312. DOI: 10.4103/0975-7406.100283.

[27] N. Gridina et al. "Surface Plasmon Resonance Biosensor". In: *Sensors and Transducers* 149.2 (2013), pp. 60–68.

[28] H. Guner et al. "A smartphone based surface plasmon resonanc eimaging (SPRi) platform for on-site biodetection". In: *Sensors and Actenuators B: Chemical (Elsevier)* 239 (2017), pp. 571–577. DOI: 10.1016/j.snb.2016.08.061.

[29] P. Guo et al. "Isolation and Characterization of Petroleum Hydrocarbon Degrading Bacteria from the Bohai Sea, China". In: *Advanced Materials Research* 955-959 (2014), pp. 728–731. DOI: 10.4028/www.scientific.net/AMR.955-959.728.

[30] A. Hara, K. Syutsubo, and S. Harayama. "Alcanivorax which prevailsin oil-contaminated seawater exhibits broad substrate specificity for alkane degradation". In: *Environmental Biology* 5.9 (2003), pp. 746–753. DOI: 10.1046/j.1462-2920.2003.00468..

[31] S. Harayama, Y. Kasai, and A. Hara. "Microbial communities in oil-contaminated seawater". In: *Current opinion in Biotechnology* 15 (2004), pp. 205–214. DOI: 10.1016/j.copbio.2004.04.002.

[32] S. Harayama et al. "Petroleum Biodegradation in Marine Environments". In: *JMMB Symposium*. Vol. 1. Journal of Molecular Microbiology and Biotechnology, 1999, pp. 63–70.

[33] T. H. Hazen et al. "Deep-Sea Oil Plume Enriches Indigenous Oil-Degrading Bacteria". In: *Science* 330.6001 (2010), pp. 204–208. DOI: 10.1126/science.1195979.

[34] Z. He et al. "GeoChip: a comprehensive microarray for investigating biogeochemical, ecological and environmental processes". In: *International Society for Microbial Ecology* 1 (2007), pp. 67–77.

[35] C. Howe, T. M. Fromhold, and N. A. Russell. *Surface plasmon resonance on gold microstructures*. 2018. DOI: 10.1117/12.2300953. URL: https://doi.org/10.1117/12.2300953.

[36] W. Hu et al. "Advancement of Nucleic Acid Biosensors Based on Morpholino". In: *American Journal of Biomedical Science* 7.1 (2015), pp. 40–51. DOI: 10.5099/aj150100040.

[37] J. Janda and S. Abott. "16S rRNA Gene Sequencing for Bacterial Identification in the Diagnostic Laboratory: Pluses, Perils, and Pitfalls". In: *Journal of Clinical*

Microbiology (American Society for Microbiology) 45.9 (2007), pp. 2761–2764. DOI: 10.1128/JCM.01228-07.

[38] C. Justino et al. "Sensors and biosensors for monitoring marine contaminants". In: *Trends in Environmental Analytical Chemistry* 6.7 (2015), pp. 21–30. DOI: 10.1016/j.teac.2015.02.001.

[39] Celine I. L. Justino, Armando C. Duarte, and Teresa A. P. Rocha-Santos. "Recent Progress in Biosensors for Environmental Monitoring: A Review". In: *sensors* 17 (2017). DOI: 10.3390/s17122918.

[40] Adriana Królicka et al. "Detection of Oil Leaks by Quantifying Hydrocarbonoclastic Bacteria in Cold Marine Environments Using the Environmental Sample Processor". In: *ResearchGate*. July 2014.

[41] S. Kröger and R. Law. "Biosensors for marine applications. We all need the sea, but does the sea need biosensors?" In: *Biosensors & Bioelectronics* 20 (2005), pp. 1903–1913. DOI: 10.1016/j.bios.2004.08.036.

[42] Guan Chin Kuan et al. "Gold-nanoparticle based electrochemical DNA sensor for the detection of fish pathogen Aphanomyces invadans". In: *Talanta* 117 (2013), pp. 312–317.

[43] M. Kube et al. "Genome sequence and functional genomic analysisof the oil-degrading bacterium Oleispira antarctica". In: *Nature communications* 4.2156 (2013). DOI: 10.1038/ncomms3156.

[44] J. Leahy and R. R. Colwell. "Microbial Degradation of Hydrocarbons in the Environment". In: *Microbiological Reviews* 54.3 (1990), pp. 305–315.

[45] Rastislav Levicky, Ursula Koniges, and Napoleon Tercero. "Diagnostic Applications of Morpholinos and Label-Free Electrochemical Detection of Nucleic Acids". In: *Morpholino Oligomers: Methods and Protocols*. Ed. by Hong M. Moulton and Jon D. Moulton. Vol. 10. 1565. New York, NY: Springer New York, 2017, pp. 181–190. ISBN: 978-1-4939-6817-6. DOI: 10.1007/978-1-4939-6817-6_15. URL: https://doi.org/10.1007/978-1-4939-6817-6_15.

[46] Y. Li et al. "Single Nucleotide Polymorphism Genotyping by Nanoparticle-Enhanced SPR Imaging Measurements of Surface Ligation Reactions". In: *Analytical Chemistry* 78.9 (2006), pp. 3158–3164.

[47] C. Liu et al. "Electrochemical detection of Pseudomonas aeruginosa 16S rRNA using a biosensor based on immobilized stem–loop structured probe". In: *Enzyme and Microbial Technology* 49 (2011), pp. 266–271.

[48] J. Liu et al. "Proliferation of hydrocarbon-degrading microbes at the bottom of the Mariana Trench". In: *Microbiome* 7.1 (2019), p. 47. ISSN: 2049-2618. DOI: 10.1186/s40168-019-0652-3. URL: https://doi.org/10.1186/s40168-019-0652-3.

[49] A. P. Luz et al. "A survey of indigenous microbial hydrocarbon degradation genes in soils from Antarctica and Brazil". In: *Canadian Journal of Microbiology* 50.5 (2004), pp. 323–333. DOI: 10.1139/W04-008.

[50] A. Manti, S. Papa, and P. Boi. "What Flow Cytometry can Tell Us About Marine Micro-Organisms – Current Status and Future Applications". In: ed. by I. Schmid. InTech, 2012. Chap. 1, pp. 1–28. ISBN: 978-953-51-0626-5.

[51] C. L. Manzanares-Palenzuela et al. "Electrochemical genosensors as innovative tools for detection ofgenetically modified organisms". In: *Trends in Analytical Chemistry* 66 (2015), pp. 19–31. DOI: 10.1016/j.trac.2014.10.006.

[52] A. G. Marshall and A. P. Rodgers. "Petroleomics: The Next Grand Challenge for Chemical Analysis". In: *Accounts of Chemical Research* 37 (2004), pp. 53–59.

[53] O. U. Mason et al. "Metagenome, metatranscriptome and single-cell sequencing reveal microbial response to Deepwater Horizon oil spill". In: *The ISME Journal (International Society for Micriobiolic Ecology)* 6 (2012), pp. 1715–1727. DOI: 10.1038/ismej.2012.5.

[54] J. Clerk Maxwell. "A Dynamical Theory of the Electromagnetic Field". In: *Philosophical Transactions* 155 (1864), pp. 459–512.

[55] T. J. McGenity et al. "Marine crude-oil biodegradation: a central role for interspecies interactions". In: *Aquatic Biosystems* 8.10 (2012). DOI: 10.1186/2046-9063-8-10. URL: http://www.aquaticbiosystems.org/content/8/1/10.

[56] B. A. McKew et al. "Determining the identity and roles of oil-metabolizing marine bacteria from the Thames estuary, UK". In: *Environmental Microbiology* 9.1 (2007), pp. 165–175. DOI: 10.1111/j.1462-2920.2006.01125.x.

[57] L. K. Medlin and J. Orozco. "Molecular Techniques for the Detection of Organisms in Aquatic Environments, with Emphasis on Harmful Algal Bloom Species". In: *Sensors* 17.5 (2017). DOI: 10.3390/s1705118.

[58] J. Michel, G. Shigenaka, and R. Hoff. "Oil Spill Response and Cleanup Techniques". In: An Introduction to Coastal Habitats and Biological Resources for Oil Spill Response. Hazardous Materials Response, Assessment Division National Oceanic, and Atmospheric Administration 7600 Sand Point Way NE Seattle, Washington 98115: National Oceanic and atmospheric administration. U.S. Department of commerce, 1992. Chap. 5, pp. 219–323. URL: http://wildpro.twycrosszoo.org/000ADOBES/NOAAMontereyD162/chapter5.pdf.

[59] T. Miyatake, B. J. MacGregor, and H. T. S. Boschker. "Linking Microbial Community Function to Phylogeny of Sulfate-Reducing Deltaproteobacteria in Marine Sediments by Combining Stable Isotope Probing with Magnetic-Bead Capture Hybridization of 16S rRNA". In: *Applied and Environmental Microbiology* 75.15 (2009), pp. 4927–4935. DOI: 10.1128/AEM.00652-09.

[60] Monterey Bay Aquarium Research Institute. *The Environmental Sample Processor (ESP)*. Internet. 2019. URL: https://www.mbari.org/technology/emerging-current-tools/instruments/environmental-sample-processor-esp/.

[61] National Research Council. *Oil in the sea III, Inputs, Fates and Effects*. The National Academies Press, 2003. DOI: 10.17226/10388.

[62] T. A. Nelson et al. "PhyloChip microarray analysis reveals altered gastrointestinal microbial communities in a rat model of colonic hypersensitivity". In: *Neurogastroenterology & Motility* 23.2 (2011), pp. 169–177. DOI: 10.1111/j.1365-2982.2010.01637.x. URL: https://onlinelibrary.wiley.com/doi/abs/10.1111/j.1365-2982.2010.01637.x.

[63] Nicoyalife. *Reducing Non-Specific Binding in Surface Plasmon Resonance Experiments*. Accessed 2018-01. Nov. 2015. URL: https://www.nicoyalife.com/wp-content/uploads/2015/11/Reducing-Non-Specific-Binding-in-Surface-Plasmon-Resonance-Experiments.pdf.

[64] Y. Nie et al. "Diverse alkane hydroxylase genes in microorganisms and environments". In: *Scientific Reports* 4.4968 (2014). DOI: 10.1038/srep04968.

[65] J. Orozco and L. K. Medlin. "Electrochemical performance of a DNA-based sensor device for detecting toxic algae". In: *Sensors and Actuators B: Chemical (Elsevier)* 153 (2010), pp. 71–77. DOI: 10.1016/j.snb.2010.10.016.

[66] Ilaria Palchetti and Marco Mascini. "Nucleic acid biosensors for environmental pollution monitoring". In: *The Analyst* 133.7 (2008), pp. 846–854. DOI: 10.1039/b802920m.

[67] Daniela M. Pampanin and Magne O. Sydnes. "Polycyclic Aromatic Hydrocarbons a Constituent of Petroleum: Presence and Influence in the Aquatic Environment". In: *Hydrocarbon*. Ed. by Vladimir Kutcherov and Anton Kolesnikov. Rijeka: IntechOpen, 2013. Chap. 5. DOI: 10.5772/48176. URL: https://www.intechopen.com/books/hydrocarbon/polycyclic-aromatic-hydrocarbons-a-constituent-of-petroleum-presence-and-influence-in-the-aquatic-en.

[68] Douglas Pargett et al. "Development of a Mobile Ecogenomic Sensor". In: *OCEANS 2015 - MTS/IEEE Washington*. Oct. 2015, pp. 1–6. DOI: 10.23919/OCEANS.2015.7404361.

[69] R. Peltomaa et al. "Optical Biosensors for Label-Free Detection of Small Molecules". In: *Sensors* 18.12 (2018), p. 4126. DOI: 10.3390/s18124126.

[70] K. Porter and Y. S. Feig. "The use of DAPI for identifying and counting aquatic microflora". In: *Limnology and Oceanography* 25.5 (1980), pp. 943–948. DOI: 10.4319/lo.1980.25.5.0943.

[71] C. M. Preston et al. "Near real-time, autonomous detection of marine bacterioplankton on a coastal mooring in Monterey Bay, California, using rRNA-targeted DNA probes". In: *Environmental Biology* 11.5 (2009), pp. 1168–1180. DOI: 10.1111/j.1462-2920.2009.01848.x.

[72] Christina M. Preston et al. "Underwater Application of Quantitative PCR on an Ocean Mooring". In: *PLoS ONE* 6.8 (2011). DOI: 10.1371/journal.pone.0022522.

[73] D. Quesada-Gonzalez and A. Merkoci. "Mobile phone-based biosensing: An emerging"diagnostic andcommunication"technology". In: *Biosensors and Bioelectronics* 92 (2017), pp. 549–562. DOI: 10.1016/j.bios.2016.10.062. URL: http://dx.doi.org/10.1016/j.bios.2016.10.062.

[74] F. Rojo. "Enzymes for Aerobic Degradation of Alkanes". In: ed. by K. N. Timmis. Springer-Verlag Berlin Heidelberg, 2010. Chap. 3, pp. 781–797. DOI: 10.1007/978-3-540-77587-4_59.

[75] J. Sabirova et al. "Proteomic Insights into Metabolic Adaptations in Alcanivorax borkumensis Induced by Alkane Utilization". In: *Journal of Bacteriology (American Society for Microbiology)* 188.11 (2006), pp. 3763–3773. DOI: 10.1128/JB.00072-06.

[76] J. R. Sambles, G. W. Bradbery, and F. Yang. "Optical excitation of surface plasmons: A Review". In: *Contemporary Physics* 32.3 (1991), pp. 173–183.

[77] C. A. Scholin. "What are "ecogenomic sensors?" A review and thoughts forthe future". In: *Ocean Science* 6.1 (2010), pp. 191–213. DOI: 10.5194/osd-6-191-2009.

[78] E. Sevilla, L. Yuste, and F. Roj. "Marine hydrocarbonoclastic bacteria as whole-cell biosensors for n-alkanes". In: *Microbial Biotechnology* 8.4 (2015), pp. 693–706. DOI: 10.1111/1751-7915.12286.

[79] S. D. Soelberg et al. "A portable surface plasmon resonance sensor system for real-time monitoring of small to large analytes". In: *Journal of Industrial Microbiology and Biotechnology (Society of Industrial Microbiology)* 32 (2005), pp. 669–674. DOI: 10.1007/s10295-005-0044-5.

[80] C. Suparpprom et al. "Synthesis and oligodeoxynucleotide binding properties of pyrrolidinyl peptide nucleic acids bearingprolyl-2-aminocyclopentanecarboxylic acid (ACPC) backbones". In: *Tetrahedon Letters (Elsevier)* 46 (2005), pp. 833–837. DOI: 10.1016/j.tetlet.2005.02.126.

[81] S. Sutton. "The Most Probable Number Method and Its Uses in Enumeration, Qualification, and Validation". In: *Journal of Validation Technology* 16.3 (2010), pp. 35–38.

[82] H. Sípová and J. Homola. "Surface plasmon resonance sensing of nucleic acids: A review". In: *Analytica Chimica Acta (Elsevier)* 773 (2013), pp. 9–23. DOI: 10.1016/j.aca.2012.12.040.

[83] Y. Tang, X. Zeng, and J. Liang. "Surface Plasmon Resonance: An Introduction to a Surface Spectroscopy Technique". In: *Journal of Chemical Education* 87 (2010), pp. 742–746. DOI: 10.1021/ed100186y.

[84] Y. Tapilatu et al. "Isolation of alkane-degrading bacteria from deep-sea Mediterranean sediments". In: *Letters in Applied Microbiology* 50 (2009), pp. 234–236. DOI: 10.1111/j.1472-765X.2009.02766.x.

[85] N. Tercero et al. "Hybridization, Morpholino Monolayers: Preparation and Label-Free DNA Analysis by Surface Hybridization". In: *Journal of American Chemical Society* 131.13 (2009), pp. 4953–4961. DOI: 10.1021/ja810051q.

[86] University of Vienna. *Vienna RNA Web Servers*. Accessed 2019-02-14. 2019. URL: http://rna.tbi.univie.ac.at/cgi-bin/RNAWebSuite/RNAfold.cgi?PAGE=3&ID=lClRoBZ9zY.

[87] A. Valoczi et al. "Sensitive and specific detection of microRNAs by northern blot analysis using LNA-modified oligonucleotide probes". In: *Nucleic acids Research* 32.22 (2004), p. 175. DOI: 10.1093/nar/gnh171.

[88] S. J. Varjani. "Microbial degradation of petroleum hydrocarbons". eng. In: *Bioresource Technology* 223 (2017), pp. 277–286. ISSN: 0960-8524. DOI: 10.1016/j.biortech.2016.10.037.

[89] A. P. Vinogradov et al. "Exciting surface plasmon polaritons in the Kretschmann configuration by light beam". In: *American Physical Society* 97.23 (2018). DOI: 10.1103/PhysRevB.97.235407.

[90] F. Wang et al. "GeoChip-based analysis of metabolic diversity of microbial communities at the Juan de Fuca Ridge hydrothermal vent". In: *PNAS* 106.12 (2009), pp. 4840–4845.

[91] M. M. Yakimov, K. N. Timmis, and P. N. Golyshin. "Obligate oil-degrading marine bacteria". In: *Current opinion in Biotechnology (Elsevier)* 18 (2007), pp. 257–266. DOI: 10.1016/j.copbio.2007.04.006.

[92] M. M. Yakimov et al. "Oleispira antarctica gen. nov., sp. nov., a novel hydrocarbonoclastic marine bacterium isolated from Antarctic coastal sea water". In: *International Journal of Systematic and Evolutionary Microbiology* 53 (2003), pp. 779–785. DOI: 10.1099/ijs.0.02366-0.

[93] F. Yu, D. Yao, and W. Knoll. "Oligonucleotide hybridization studied by a surface plasmon diffraction sensor (SPDS)". In: *Nucleic Acid Research* 32.9 (2004). DOI: 10.1093/nar/gnh067.

[94] E. Yılmaz et al. "Plastic antibody based surface plasmon resonance nanosensors forselective atrazine detection". In: *Materials Science and Engineering C* 73 (2017), pp. 603–610. DOI: 10.1016/j.msec.2016.12.0900928-4931.

[95] F. Zezza et al. "Detection of Fusarium culmorum in wheat by a surface plasmon resonance-based DNA sensor". In: *Journal of Microbiological Methods* 66.3 (2006), pp. 529–537. DOI: 10.1016/j.mimet.2006.02.003.

[96] Q. Zhang et al. "Surface plasmon resonance sensor for femtomolar detection of testosterone with water-compatible macroporous molecularly imprinted film". In: *Analytical Biochemistry* 463 (2014), pp. 7–14. DOI: 10.1016/j.ab.2014.06.0140003-2697.